NTNU
Det skapende universitet

Kompakt 3dB kvadratur-kobler implementert i MMIC

Houman Mohebbi

Master i kommunikasjonsteknologi
Oppgaven levert: Juli 2007
Hovedveileder: Morten Olavsbråten, IET
Biveileder(e): Kjetil Folgerø, Nera Networks

Norges teknisk-naturvitenskapelige universitet
Institutt for elektronikk og telekommunikasjon

Oppgavetekst

Koblere er viktige komponenter i oppbygningen av radiosystem, hvor en skal splitte eller kombinere signaler. Oppbygningen av en kobler er tradisjonelt
gjort med transmisjonslinjer. Dette medfører at koblerne blir store, og egner seg derfor normalt ikke til integrasjon i MMIC.
Oppgaven vil gå ut på å:

- sette seg inn i bruk av kretssimulatoren ADS og EM simulatoren Momentum.
- sette seg inn i Triquints MMIC prosess.
- Utføre målinger på tidligere produserte MMIC komponenter og sammenligne disse med kretssimulering og EM simulering av samme komponent.
- vurdere ulike topologier av 3dB kvadratur-koblere for implementasjon i MMIC, ut fra litteratursøk og innledende simuleringer.
- designe aktuelle koblere i MMIC

Oppgaven gitt: 19. januar 2007
Hovedveileder: Morten Olavsbråten, IET

Compact 3dB quadrature coupler implemented in MMIC

by Houman Mohebbi

Department of Electronics and Telecommunications

Abstract

In this thesis different design techniques for compact 3dB quadrature hybrids, operating in the frequency range 5-10 GHz, is described. Methods are given for arbitrary impedance terminations, center frequency and bandwidth. The proposed quadrature hybrids are realized using TriQuint HBT3 MMIC process. The MMIC circuits make use of transmission lines, spiral inductors and MIM capacitors. Simulated data for different couplers are provided and discussed. Coupler size reduction techniques are described and carry through with an achieved size reduction larger than 71% compared with conventional transmission line branch-line coupler. EM- and circuit-simulations of passive MMIC have been carried out and compared with experimental results to validate the use of foundry models with real life measurements.

Acknowledgments

I would like to express my gratitude to my teaching supervisor Associate Professor Morten Olavsbråten for his continuous guidance and readiness to help during my work. I want to thank the Department of Electronics and Telecommunications and Nera Networks AS for giving me the opportunity to write this thesis. Further I would like to thank Kjetil Folgerø who was my supervisor at Nera Networks for defining the task and helping me during this time. I would also like to thank research engineer Terje Mathiesen for his assistance in ADS Momentum and PhD student Marius Ubostad for his help during measurements in the microwave laboratory.

Contents

List of Figures

List of Tables

Acronyms

CAD Computer Aided Design

DBS Direct broadcast satellite

EM Electro Magnetic

GaAs Gallium Arsenide

GPS Global Positioning System

HBT Heterojunction Bipolar Transistor

InP Indium Phosphide

MIC Microwave Integrated Circuits

MIM Metal-Insulator-Metal

MMIC Monolithic Microwave Integrated Circuit

MTTF Mean Time To Failure

PA Power Amplifier

PCS Personal Communication Systems

pHEMT pseudomorphic High Electron Mobility Transistor

SiGe Silicon Germanium

SRF Self Resonant Frequency

VSWR Voltage Standing Wave Ratio

WLAN Wireless Local Area Network

Chapter 1

Introduction

1.1 Motivation and Goals for Thesis

A 3dB quadrature coupler divides an input signal into two equal components with a mutual phase difference of 90 degrees. Quadrature couplers are essential components for maintaining a balanced circuit solution among other microwave components such as mixers and amplifiers. In suchlike components the coupler will terminate the reflections from the other units into a load that is isolated from the couplers input-port. This will apply good impedance matching to the balanced circuit even though the unbalanced units have poor impedance matching. In frequency mixers the coupler is used to balance out LO signals. Also unwanted sidebands can be balanced out using a quadrature coupler.

One of the main challenges when using quadrature couplers in MMIC is that the components tend to become large. Therefore the component will consume large areas of the semi-conductor area, and become expensive. Quadrature couplers have a limited bandwidth, which will result that several different couplers has to be design in order to maintain a large bandwidth.

The goal with this thesis is to investigate the adequacy of different coupler topologies with regard to compactness and performance. Important performance parameters to be examined are phase balance, amplitude balance, bandwidth and losses due to MMIC implementation. The parameters are to be weighted against compactness and design complexity.

1.2 Problem Overview

In this thesis different coupler topologies are considered from literature study and simulations will be carried out. From the simulations and literature study a methodology for designing couplers will prepared in order to design couplers

for different frequencies, bandwidths and other critical properties.

The task will be divided into several areas which are as follows:

- Gain an insight to use of the circuit simulator Agilent ADS and the EM-simulator Momentum.
- Understand and evaluate the TriQuint MMIC process.
- Perform measurements on previous manufactured MMIC components to compare with circuit simulations and EM-simulations with the same circuit setup.
- Evaluate various 3 dB quadrature coupler topologies for implementation in MMIC from literature study, and execute preliminary simulations.
- Design relevant couplers using MMIC.

1.3 Design Requirements

In order for the quadrature coupler to be evaluated some design criteria's are laid down. The frequency range and response properties reflect criterias that would make the coupler useful in current microwave applications. During the design process TriQuint pHEMT or HBT- process is used as requested by NERA Networks. Some of the requirements are listed in table 1.1. Another important factor to keep in mind is that the final chip should be as compact as possible which will act as a bottle neck in the design. When minimizing the design many effects such as coupling between components may impair the performance of the circuit.

Frequency range	5 - 10 GHz
Bandwidth	$> 30\%$
Phase balance	< 5deg
Amplitude balance	$<$0.5dB
Design process	TriQuint pHEMT or HBT process
Substrate	GaAs

Table 1.1: Design properties

Chapter 2

Coupler Theory

2.1 Couplers and its Applications

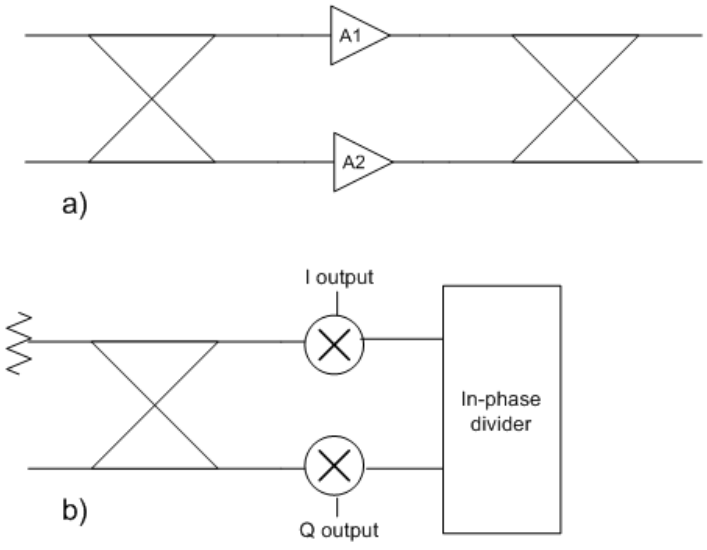

Figure 2.1: Schematic illustration of a) balanced amplifier and b) IQ demodulator , [1]

Couplers are passive microwave devices often used for power division or power combining. Couplers can be divided into to main groups, three-ports and four-ports, respectively known as T-junctions and directional couplers. T-

junctions are often used as equal power dividers, while directional couplers are designed for both equal (hybrids) and unequal power division. With directional couplers we can have phase shift at the output ports, either 90° (quadrature) or 180° (magic-T). When we refer to directional coupler as a *quadrature hybrid* it means that the coupler has an equal power split (3dB) and 90° phase shift between the output ports [12]. This thesis concentrates around four-ports, therefore three-port theory is not examined.

Directional couplers have many applications in microwave circuits. It is often used to balance circuits. Balanced amplifiers employs quadrature hybrids in order to compensate with mis-matching and to improve the amplifier linearity. A balanced amplifier,fig 2.1a), often achieves a broad bandwidth with flat gain and good Voltage Standing Wave Ratio (VSWR), [2]. Also numerous circuits such as phase shifters, balanced mixers, image reject mixers and IQ demodulators, fig 2.1b), make use of quadrature hybrids for different purposes. Detailed descriptions on these circuits can be found in Andrews [1].

2.2 Directional Coupler Theory

The properties of the coupler is to divide the power between two ports and have an isolated port to handle reflections that might occur from the output ports. Figure 2.2 shows a schematic illustration of a directional coupler. In this case the incident wave is at port 1. The power from port 1 is coupled into the output ports 2 and 3 and not into the isolated port 4. This is noted by arrows in the figure. If three ports are matched then the last port will also seem terminated with matched load and therefore eliminate reflections to some extent. The same rules apply if the incident are at port 2 or 3.

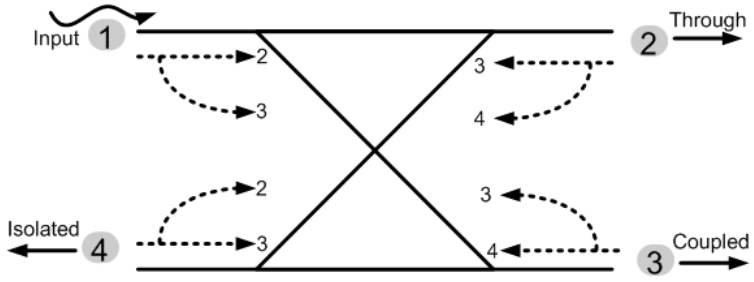

Figure 2.2: Schematic illustration of a directional coupler

The directional coupler can be expressed using a four-port scattering matrix (S-matrix) [12]. The S-matrix for a reciprocal four-port can be expressed as the matrix 2.1 (all ports matched).

$$[S] = \begin{pmatrix} 0 & S_{12} & S_{13} & S_{14} \\ S_{12} & 0 & S_{23} & S_{24} \\ S_{13} & S_{23} & 0 & S_{34} \\ S_{14} & S_{24} & S_{34} & 0 \end{pmatrix} \tag{2.1}$$

Using the properties of a directional coupler it is known that there is no coupling between port 1 and 4. The same properties exists for port 2 and 3 as well:

$$S_{14} = S_{23} = 0$$

Resulting to the S-matrix:

$$[S] = \begin{pmatrix} 0 & S_{12} & S_{13} & 0 \\ S_{12} & 0 & 0 & S_{24} \\ S_{13} & 0 & 0 & S_{34} \\ 0 & S_{24} & S_{34} & 0 \end{pmatrix} \tag{2.2}$$

From figure 2.2 it is also known that the coupling between port 1 and 3 are equal to port 2 and 4. Similarly the coupling between port 1 and 2 is equal to the coupling between 3 and 4.

$$|S_{13}| = |S_{24}|$$

$$|S_{12}| = |S_{34}|$$

By setting up the product of the first with its conjugate equals 1, and similarly with the second row we obtain:

$$|S_{12}|^2 + |S_{13}|^2 = 1 \tag{2.3}$$
$$|S_{12}|^2 + |S_{24}|^2 = 1 \tag{2.4}$$

Choosing reference point on the three of the ports, we can set $S_{12} = S_{34} = \alpha$, where α is a real. S_{13} and S_{24} on the other hand will include a phase shift, therefore we denote $S_{13} = S_{24} = \beta e^{j\Omega}$ as we assume they have the same phase shift (symmetric coupler). Since the dot product of row 2 and 3 gives $S_{12}^* S_{13} + S_{24}^* S_{34} = 0$ we have that the phase constant Ω has to be $\pi/2$ ($e^{j\pi/2}$ = j). We then obtain the final S-matrix (fig 2.5). Complete derivation can be seen using chapter 4 and 5 in [12].

$$[S] = \begin{pmatrix} 0 & \alpha & j\beta & 0 \\ \alpha & 0 & 0 & j\beta \\ j\beta & 0 & 0 & \alpha \\ 0 & j\beta & \alpha & 0 \end{pmatrix} \tag{2.5}$$

Defining this for a quadrature hybrid which has equal power split, (3dB= $\frac{1}{\sqrt{2}}$), the S-matrix can characterized by setting $\alpha = \beta = \frac{1}{\sqrt{2}}$:

$$[S] = \frac{1}{\sqrt{2}} \begin{pmatrix} 0 & 1 & j & 0 \\ 1 & 0 & 0 & j \\ j & 0 & 0 & 1 \\ 0 & j & 1 & 0 \end{pmatrix} \tag{2.6}$$

2.3 Characterization of Directional Couplers

There are three factors often used to characterize a directional coupler which are coupling, directivity and isolation.
The coupling defines the quantity of input power that is coupled to the output port. It is defined as the power relation between port 3 and port 1 if we assume port 3 to be the coupled port and port 1 as the input port. This relation can be written as:

$$Coupling(C) = 10 \log \frac{P_1}{P_3} = -20 \log \beta \ \mathbf{dB} \tag{2.7}$$

where P_1 and P_3 are input power and output power at ports 1 and 3 respectively. β is same for 2.5.

The power coupled backward into the isolation port should be 0 on a ideal coupler, e.g. $S_{14} = 0$. To measure this we use directivity. In other words directivity measures how good the power is directed in the wanted direction and defined by:

$$Directivity(D) = 10 \log \frac{P_3}{P_4} = 20 \log \frac{\beta}{|S_{14}|} \ \mathbf{dB} \tag{2.8}$$

As mentioned above S_{14} should be zero in an ideal coupler,which implies that the directivity should be infinity. Directivity is a very important factor to avoid backward leakage in many applications. Feed forward amplifiers rely strongly on this factor as reflection from for example an antenna may cause the amplifier not to function properly, [13].

Isolation of a directional coupler is defined by power from port 1(input) to port 4(isolated port) and can be expressed as:

$$Isolation(I) = 10 \log \frac{P_1}{P_4} = -20 \log |S_{14}| \ \mathbf{dB} \tag{2.9}$$

or,

$$I = (D + C) \ \mathbf{dB} \tag{2.10}$$

From the relation 2.10 it can be seen that for an ideal directional coupler the isolation should be infinite, since the ideal directivity is infinite.

One should become aware of the fact that all these factors are non constant and will vary by frequency. When we define a coupling factor it is usually for a given center frequency. The degree of variation is dependent on degree of band broadness of our circuit.

2.4 Different Quadrature Coupler Structures

There are different ways of designing quadrature couplers, depending of technology and frequency. Some of these are reviewed in this section. All of these are based on the theory in section 2.2. Waveguide couplers are often used in microwave circuits but not relevant for this paper and therefore not examined further.

Branch-Line Coupler

Branch-line couplers are often applied in planar circuits. This coupler is easily constructed using a symmetrical structure and applying quarter wave length ($\lambda/4$) lines for a characteristic impedance Z_0. A basic structure is illustrated in figure 2.3.

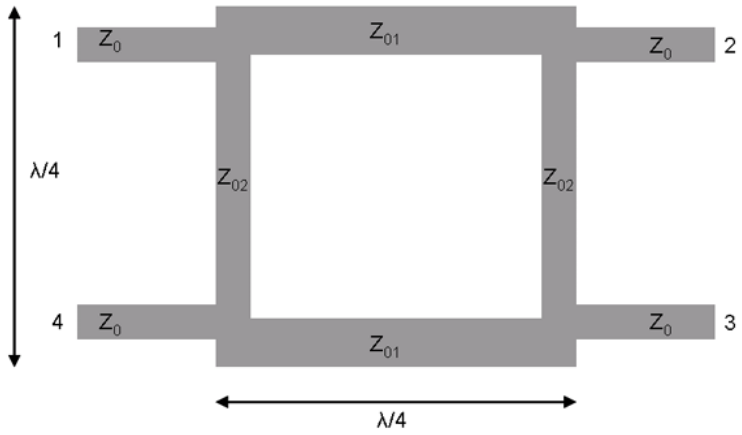

Figure 2.3: Microstrip branch-line coupler

In the figure Z_0 is the characteristic impedance, λ the wavelength at center frequency (f_0) and Z_{0i} the line impedances. The line impedances can calculated using formulas from [2] for known coupling factor in dB and characteristic impedance:

$$C = 10\ log \frac{1}{1 - \left(\frac{Z_{01}}{Z_0}\right)^2} \tag{2.11}$$

$$\frac{Z_{02}}{Z_0} = \frac{\frac{Z_{01}}{Z_0}}{\sqrt{1 - \left(\frac{Z_{01}}{Z_0}\right)^2}} \tag{2.12}$$

When the line impedances are found CAD [1] tools can be used to find the dimensions of the strip lines by defining the substrate parameters and frequency.

Coupled-Line Coupler

Figure 2.4: Coupled-line directional coupler

Coupled-line directional coupler (fig. 2.4) design is often used in planar microwave circuits as well. The coupled-line directional coupler makes use of the magnetic coupling between the lines and therefore reduces the size of the circuit. In order to calculate the lines dimensions, even- and odd- characteristic impedances has to be used. The detailed analysis can be found in [12], resulting in equations 2.13 and 2.14, where C is the coupling factor in dB.

$$Z_{0e} = Z_0 \sqrt{\frac{1 + 10^{-C/20}}{1 - 10^{-C/20}}} \tag{2.13}$$

$$Z_{0o} = Z_0 \sqrt{\frac{1 - 10^{-C/20}}{1 + 10^{-C/20}}} \tag{2.14}$$

where Z_{0e} is the even-mode impedance and Z_{0o} is the odd-mode impedance. In the same manner as the branch-line coupler it is possible to calculate line dimensions and also spacing between the lines using CAD tools such as Agilent ADS. The coupled lines for this coupler also needs to be $\lambda/4$ long to achieve the desired quadrature effect.

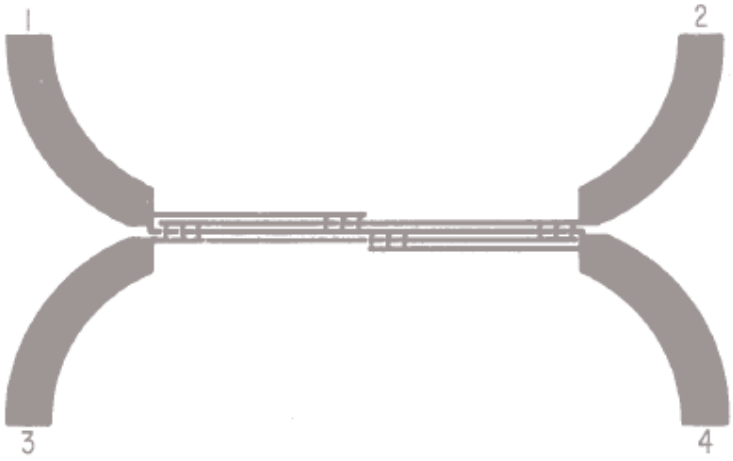

Figure 2.5: Lange coupler using planar-technology, [2]

Lange Coupler

Like the coupled-line directional coupler the Lange coupler(fig. 2.5) also employs coupling between the lines. The design was first introduced by J. Lange [14] which uses numerous tight coupled arms allowing broader bandwidth and easily constructed to achieve 3 dB coupling. Then lines are also connected with every second line as seen in the figure. The derivation of the equations can be somewhat complicated and may not always give the perfect solution because simplifications are used, as in reference [12]. From the reference the final even- and odd-impedances can be found as:

$$Z_{0e} = Z_0 \frac{4c - 3 + \sqrt{9 - 8c^2}}{2c\sqrt{(1-c)/(1+c)}} \tag{2.15}$$

$$Z_{0o} = Z_0 \frac{4c + 3 - \sqrt{9 - 8c^2}}{2c\sqrt{(1+c)/(1-c)}} \tag{2.16}$$

where $c = 10^{-C/20}$. Again here we have to use CAD tools to find the widths and spacing of the lines for a given substrate and frequency. As said earlier the equations in Pozar [12] gives approximate results, a more thorough method can be found using equations in [15]. These equations also take into account the even number of strips or arms for the coupler. Some CAD programs have built in models for Lange couplers using microstrip and other planar technologies. Good models for MMIC are not yet implemented and therefore require the designer to design it manually, which is a complex and time consuming operation.

[1]LineCalc tool in Agilent ADS can be used for calculating line dimensions.

Lumped Element Quadrature Coupler

The couplers mentioned above require on lengthy distributed, $\lambda/4$-lines, which for low frequencies will result in lengthy lines. Coupler structures like the Lange coupler result in complex structures and can be difficult to realize using MMIC -technology, since the line dimensions and spacing will not be feasible.
Therefore it is necessary to use lumped elements to both reduce size and complexity of the design. Unlike the other coupler designs lumped element quadrature hybrids do not follow a specific design recipe. It can be realized using different topologies and design methods. An easy approach of design is based on a lumped version of the branch-line coupler, shown in figure 2.6. Lumped element hybrids can also be designed by combining lines and lumped elements in circuits where this might be an advantage. In this case we will achieve a wider bandwidth and no longer require $\lambda/4$-lines. An example of a mixed lumped element hybrid can be seen in figure 2.7.

Since there are different topologies regarding lumped element quadrature hybrids some topologies found in different literatures and articles will be reviewed in later chapter.

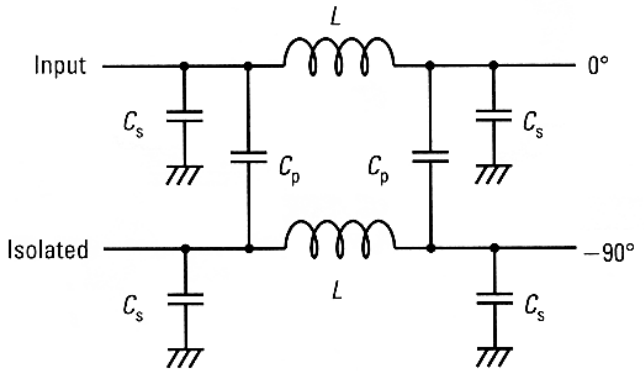

Figure 2.6: Lumped element version of a branch line coupler from [1]

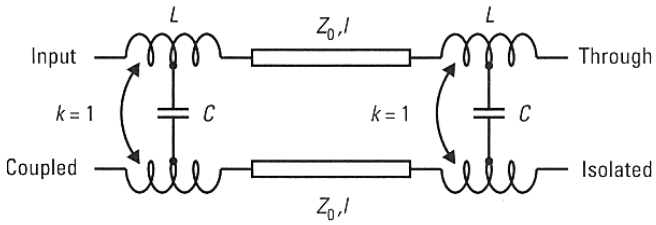

Figure 2.7: Mixed element hybrid, [1]

Chapter 3

MMIC Technology

3.1 Introduction to MMIC

Monolithic Microwave Integrated Circuit (MMIC) is a process where the active and passive components are fabricated on the same semi-conductor substrate. MMIC allows making miniature microwave components as well as a complete system on chip for microwave applications. MMIC are suited for use in the frequency range 1 to 100 GHz, [6]. Although, the applicable frequency range may vary for different components and dependent of the technology used for the design. Some MMIC-applications can also be used up to 300 GHz, but is quite rare.

It is important to distinguish between MIC and MMIC, where the former acronym stands for Microwave Integrated Circuit which is a composition of passive and active components which are soldered upon the same substrate. MICs are also known as hybrid MIC because because of the way it is composed. As mentioned before MMIC-circuits have both active and passive components made in the same substrate. This is done by applying different layers of metal, dielectrics, insulators and other alloys on the substrate. An example of an MMIC cross section is displayed in figure 3.1. The figure shows the different layers of the MMIC-circuit that might be used. This particular process is fabricated using a Gallium Arsenide (GaAs) semiconductor substrate, which is one of the most popular substrates used to develop MMIC-circuits. Other substrates which are commonly used are Indium Phosphide (InP) and Silicon Germanium (SiGe). The use of SiGe is currently emerging and is becoming a direct competitor to GaAs. In section 3.2.5 a brief comparison of these competing technologies are discussed.

MMIC chips are produced using wafers that can hold hundreds of chips depending on the size of the components on it. A normal wafer size is about 100mm-150mm diameter, so the amount of chips on a wafer will depend on

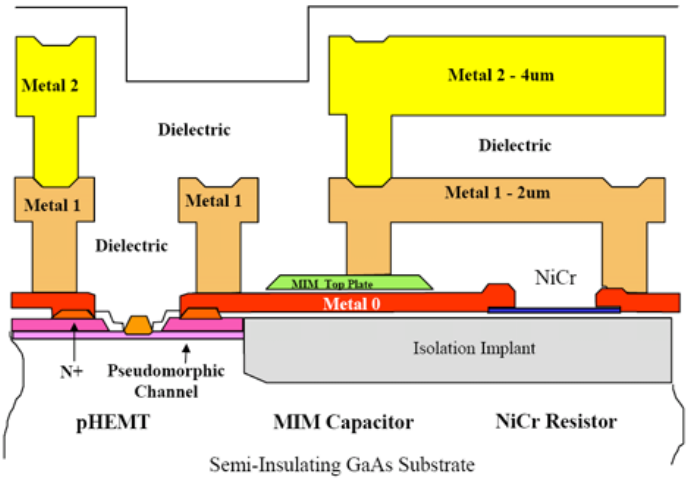

Figure 3.1: Cross section of TriQuint pHEMT process, [3]

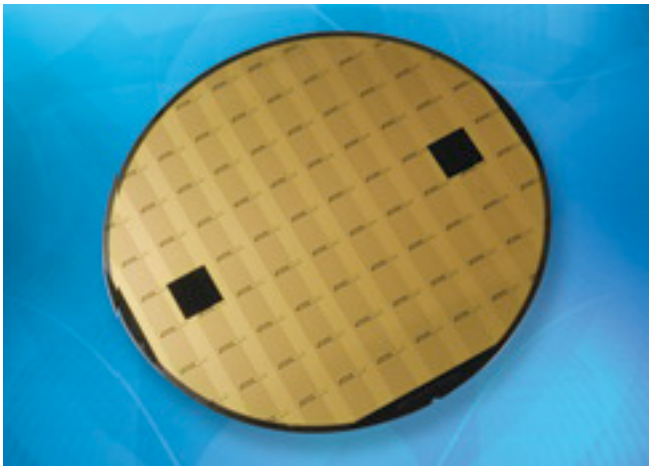

Figure 3.2: TriQuint Wafer, [4]

the chip size, which can be 1x1mm to 10x10mm. In order to make chip costs profitable one should fill the wafers as much as possible. An example of a wafer can be seen in figure 3.2.

3.2 Advantages and Disadvantages of MMICs

This section touches upon some of the strengths and weaknesses of GaAs MMIC chips compared with some of its competitors. The existing technology which

MMIC replaces is hybrid MIC, mentioned briefly in previous section. Therefore in is natural to measure the qualities of MMIC with hybrid MICs. The numbers and facts used in this comparison are taken from Robertson [6] and might be somewhat out of date, but still gives an indication of its qualities.
Later a short summary of some drawbacks and advantages when introducing SiGe semiconductors against GaAs.

3.2.1 Cost

Like any other microwave devices the cost of the components are of high importance. The price of each chip is dependent on the price of the wafer. In other words if the size of the chip decreases the price of each chip will decrease because we allow larger number of circuits per wafer. Therefore making compact components are of essence as within this thesis. If the purpose is to build few chips hybrid MICs will be much cheaper. The most considerable cost factor between hybrid MICs and MMIC are the cost of the transistors. When using hybrid MIC it is possible use transistors from other manufacturers and therefore a bigger freedom of customizing the circuit to become as cheap as possible. On the other hand this might cause some insecurity regarding the performance of the chip, more details in section 3.2.2. Another element of cost is that developing MMIC circuits are quite expensive to start up. In short terms using MMIC circuits will result in cost reduction for medium and large scale production volumes. In table 3.1[1] an estimate of how the size of each chip determines the price.

Chip Size [mm^2]	# Chips per wafer	Bare chip cost at \$9k per wafer
1	7854	1,15
4	1963	4,58
9	873	10,31
16	491	18,33
25	314	28,66
36	218	41,28
49	160	56,25
64	123	73,17
81	97	92,78
100	79	113,92

Table 3.1: Estimate of chip cost for extra wafers produced (100 mm wafer)

3.2.2 Performance

The performance of MMIC varies between manufacturers, but most of the issues regarding performance is related to use of transistors. Passive components

[1] Note that the first wafer is not considered in this estimate. The production of the first Wafer may cost \$30k and above.

tend to give quite satisfying results, even though some passive components are can consume too much space. As MMIC circuits are customized for volume production it is not to expect top performance. Although one can expect similar performance for all the chips on each wafer. As stated in 3.2.1 with hybrid MIC a designer can choose components from different manufacturers, giving the designer the liberty of utilizing components for a specific task. On the other hand MMIC can be employed in millimeter-wave applications, above 30 GHz. Unlike hybrid circuits MMIC does not allow tuning by adjusting the lumped elements on the circuit since the passive components are formed on the substrate. By having all the MMIC components on the substrate we eliminate parasitics caused by junctions, solder pads and packing which are used in hybrid circuits, hence better performance.

3.2.3 Reliability

Reliability is an important when designing microwave circuits. MMIC circuits do not have junctions in the same matter as hybrid circuits and is therefore less dependent on the reliability of each and every component. The most important criteria to assure reliability is that the fabrication process is carefully controlled and qualified. To better achieve good performance and higher reliability the designer should include manufacturing tolerances in the simulations. Again most of the reliability issues in MMIC components are regarding the transistors since the Mean Time To Failure (MTTF) of circuit depends highly on the transistors used.

MMIC circuits are today used in many applications such as WLAN, PCS, DBS, GPS and mobile technology. These are large high-volume commercial markets where reliability are of importance as well as manufacturing at consumer prices. This is a trade off which designers have to struggle with. More on this can be found in [16] and [17].

3.2.4 Size and Mass

As stated several times size important when designing MMIC circuits. MMIC components have the advantage of being both lighter and smaller then many other circuit types such as hybrid circuits. Since MMIC designs allow to make all components on the same substrate it is possible to design a complete system on the same compact chip. Therefore MMIC is relevant for use in miniaturized components such as small mobile devices. Chip sizes can vary from 1x1mm and up.

3.2.5 GaAs vs. SiGe

As mentioned the development of SiGe technology is challenging GaAs. The first thing that comes to mind is again the price. This chips are to be used for consumer electronics which require low-cost chips. In table 3.2 a cost estimate

is given, the numbers are taken from [18]. As can be seen from the table SiGe HBT gives four times lower cost per mm^2 than GaAs HBT.

Item	GaAs HBT	SiGe HBT	Units
Feature Size	2.0	0.5	μm
Starting Material	600	200	\$
Mask steps	14	28	
Photo cost	1400	2800	\$
Raw cost	2000	3000	\$
Wafer Diameter	100	200	mm
Yield	70	95	%
Cost/mm^2	0.36	0.10	\$/mm^2

Table 3.2: GaAs and SiGe RFIC cost estimates

The second most important factor is of course the performance. On this area GaAs has a leading role. GaAs has a lower field mobility than silicon. GaAs has higher saturated electron velocity, hence faster devices. This and the ability maintain low-field mobility gives GaAs an advantage when used in cellular applications and other mobile technologies where processes has to happen fast. It is in the field of Power Amplifier (PA) where these to competitors are quite similar up a given frequency. Both technologies have similar gain and noise properties, [18]. As GaAs allows quite high resistivity it is more suitable for microwave components than SiGe. All in all GaAs has been developed for a longer period of time and will continue to have a leading role versus SiGe, all though SiGe will challenge GaAs more and more in the future.

Chapter 4

Passive MMIC components

4.1 Introduction to Passive MMIC Components

Since a quadrature hybrid is a passive circuit it is necessary to evaluate the different individual components to know their response in order to properly construct the circuit. Passive components that are relevant to coupler design will be reviewed with description, equivalent models and simulations. It is also important to note that the responses and component configurations varies depending on the fabrication process. TriQuint HBT-process is evaluated in this case.

4.2 MIM Capacitors

Capacitors are essential for use in lumped element hybrids. There are two main types of MMIC capacitors, Metal-Insulator-Metal (MIM) capacitors and inter digital capacitors. TriQuint HBT process does not offer interdigital capacitors, therefore further details about this type of capacitor is not discussed.
The MIM capacitors consist of a two metal layers and separated by an insulator material, which in the case of our process is a high ϵ_r silicon nitride layer, [3].

4.2.1 Equivalent Capacitor Model

A general equivalent model for a MIM capacitor is shown in figure 4.1. The model is based on [5], where C is the capacitance, R the losses in the capacitor, L the parasitic inductance of the metal plates and C_p the parasitic capacitance between metal and substrate. The effective capacitance of the MIM capacitor can be obtained from the reactance (X_c), formula 4.1.

$$X_c = \frac{1}{j\omega C} \tag{4.1}$$

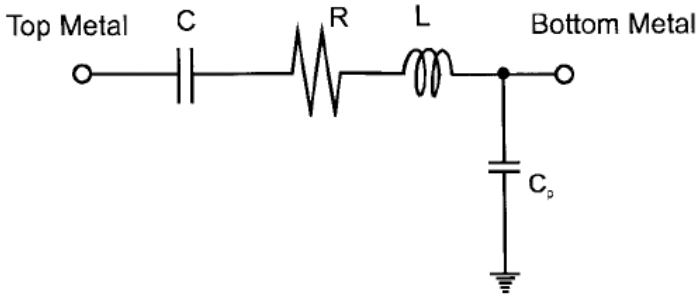

Figure 4.1: Equivalent circuit model for MIM capacitor [5]

4.2.2 Capacitor Layout Modeling using TriQuint MIM Capacitors

When we employ MIM capacitors in our design layout it is necessary to properly define the lines at the input and output of the capacitor. Since the capacitors is a multi layer component it is essential to direct the signal to the correct layer using vias and metal transmission lines. Figure 4.2 illustrates how a layout setup for a capacitor should be designed when we use metal 2 at input and output. The capacitor configuration and layer parameters can be found in [3] and Appendix A, respectively.

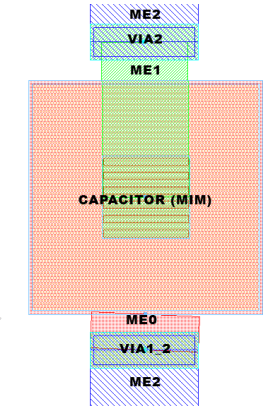

Figure 4.2: Capacitor layout model in Agilent ADS

VIA2 represents a via connection connecting metal 1 to metal 2 while VIA1_2 represents a via connection from metal 0 to metal 2. When the following component has metal0 as input it is not needed to carry the signal to a higher metal

as they can be connected directly. The same applies for metal 1. Connecting directly without vias will also result in less parasitics and unwanted responses caused by junctions, vias and line effects.

4.2.3 Simulation of a MIM capacitor

When designing circuits in ADS using equivalent schematic models it is necessary to know its response compared to what might be expected in real life. Electro Magnetic (EM)-simulations is a well known and frequently used technique that can give a hint of how the response might look when measuring in real life. Agilent ADS Momentum is a 2.5 dimensional EM-simulator used in this report. Since MMICs have a complex structure with many metal layers, dielectrics and interconnections it is an advantage to simulate using the modal characteristics and electromagnetic fields that occur within the chip.

EM-simulation setup for MIM capacitor

In order to do an EM-simulation we need to define the layers of the substrate and metal connection according to Figure 3.1 using the parameters from Appendix A. One thing to notice is that the insulating SiNx, that is the MIM dielectric, is 0.05μm thick and not as stated in the Appendix. This can be seen in article using the same technology, [19]. The final substrate definition for Momentum is shown in Fig. 4.3. Using this layer layout we may predict the measurement response to a much higher degree than regular schematic simulation.

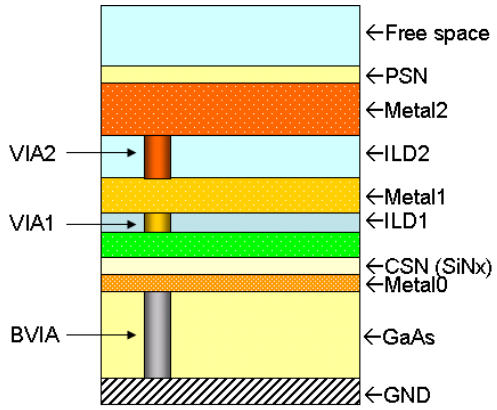

Figure 4.3: Substrate definition for Momentum simulation using MIM layers

The square MIM capacitor used in Momentum has the dimensions 65x65 μm. As stated in [19] the capacitance can be given as 1.2fF/μm^2, giving a capacitance of 5.07pF in our case. The layout in Momentum is setup with two metal2 layers at each port using the necessary vias as Figure 4.2. The complete Momentum

layout and mesh setup can be seen in Figure 4.4. The reference points of the simulation are marked with black lines. The ports are selected as single mode which is used for transmission line excitation using a calibration process that removes any undesired reactive effects of the port excitations (mode mismatch) at the port boundary, [20]. The mesh defines number of cells that layout should be divided into in order to calculate the EM-field solutions. The cells can be rectangular or polygons. A mesh of 20 is chosen, with mesh reduction turned on. The mesh reduction allows the program to reduce number cells per wavelength if the number of cells are too high. Since the MIM capacitor consists of rectangular metal layers, a 45° arc angle for the polygons should be enough. When doing EM-simulations on structures that has bends, rounded corners or other complex structures it is an advantage to use a smaller angle for the polygon cells for more accurate results. More on how EM-simulators operates can be found in Robertson [6]. The method of simulation is chosen to be adaptive sweep instead of linear. This type of sweep allows Momentum to only calculate S-parameters for the necessary frequencies by interpolating between them.

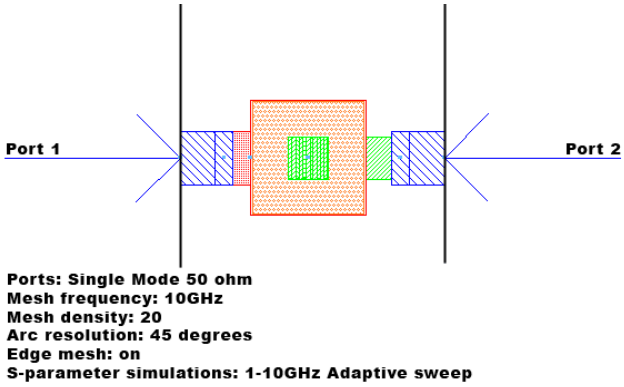

Figure 4.4: Momentum layout and mesh setup for 5pF MIM capacitor

Comparison between equivalent circuit model and EM-simulations of MIM capacitor

In order to compare the EM-simulations with the equivalent model the different transmission lines are added including the same vias used in the Momentum simulations. Microstrip transmission lines are used with the same substrate values as for GaAs, as can be seen in Figure 4.5. The simulations are done in the frequency range 1-10 GHz. The S_{21} (Fig.4.6) shows that the equivalent model for the MIM capacitor corresponds very well with the achieved results from the EM-simulations. The same applies for the S_{11} (Fig.4.7) where the difference is close to 0.2dB up to 8GHz.

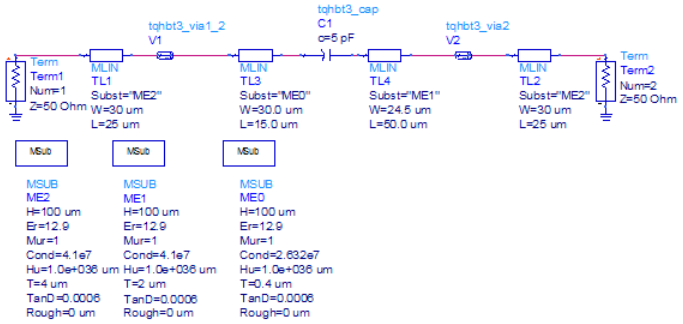

Figure 4.5: Schematic model for MIM capacitor including lines and vias

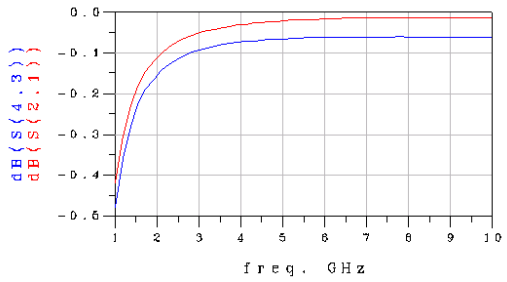

Figure 4.6: S_{21} for MIM capacitor. Equivalent model (red); EM-simulated (blue)

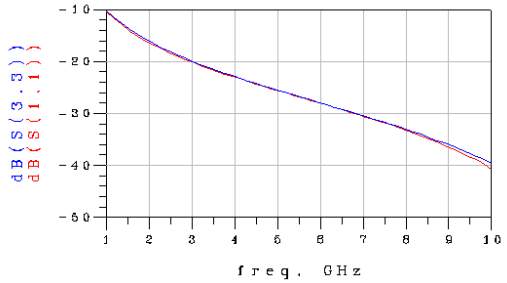

Figure 4.7: S_{11} for MIM capacitor. Equivalent model (red); EM-simulated (blue)

In order to evaluate the capacitance of the MIM capacitor the output ports are shorted making Z_{11} the input impedance. Using equation 4.1 the capacitance is obtained in Figure 4.8. The reactance is then found by taking the imaginary part of Z_{11}. The capacitance has been simulated for the frequency range 1-6GHz to see the values clearer. From the figure we see that both simulations give a capacitance $\approx$ 5pF at 1 GHz. Both simulations show that the capacitance increases with frequency. The EM-simulation of the capacitance show that it increases quicker than the equivalent model. This can be due to substrate losses and fringing fields that are taken into account when simulating in Momentum. When using the schematic model to design lumped element hybrids at the desired frequency we will get higher capacitance than desired which we must compensate by optimizing the circuit. The designer can also choose lower value capacitors in the schematic model before EM-simulating. Although one should be aware of the fact that the rate of increasing capacitance will vary between different value capacitors.

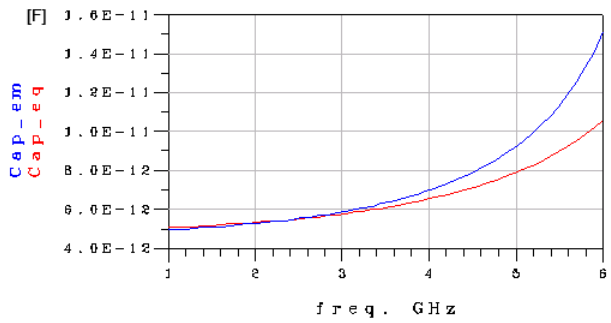

Figure 4.8: Effective capacitance of the MIM capacitor. Equivalent model (red); EM-simulated (blue)

4.3 Spiral Inductors

Inductors in MMIC are constructed in a different manner than other applications. Most common is the spiral inductor. The Spiral inductor consist of metal layers looping toward a center and then connected outside the component through air-bridges or underpasses. There are many different ways of designing the air-bridges and underpasses, some of these methods are summed up in Figure 4.9. The TriQuint tqhbt3_mrind uses a similar model as Figure 4.9 (d). The TriQuint inductor model can be constructed using Metal1, Metal2 or stacked Metal1 and Metal2 structures,[3]. The layer parameters are found in Appendix A. Different inductors can be constructed by varying the widths of the conductors, spacing between the conductors, size of the inductor, number of quarter turns and the width of the underpass conductor. Therefore it is possible to design the inductors in numerous ways.

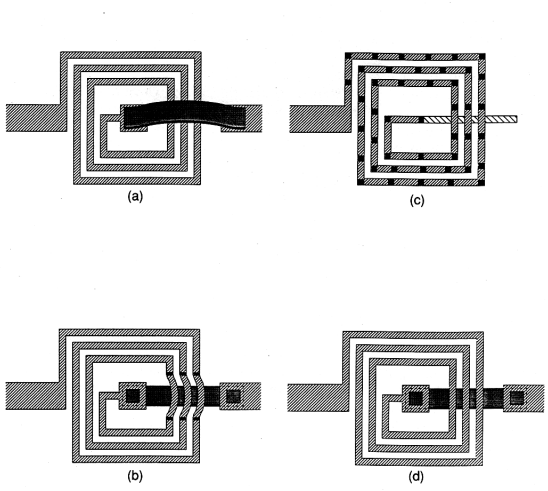

Figure 4.9: Spiral Inductors: (a) single air-bridge, (b) air-bridges over an underpass, (c) formed entirely of air-bridges, (d) using two metal levels for an underpass ; [6]

4.3.1 Equivalent Inductor Model

When exploring the inductor model (hbt3_dind) in the TriQuint Design Kit one can find the equivalent model for the spiral inductor, seen in Figure 4.10. In the figure Cout is the parasitic shunt capacitance to ground on the outside end, Ccen is the parasitic shunt capacitance to ground in the center end, the resistive losses is noted as series resistance R and L the inductance, [3]. Together with the design kit TriQuint has supplied a DOS based program, **induct_fndy.exe**, to calculate the equivalent circuit parameters. In order to obtain the total

inductance of the spiral inductor it a simulation has to be done by calculating the input impedance (Z_{in}) of the circuit. The effective inductance can then be found by the formula 4.2, where X_L is the reactance (imaginary part of Z_{in}).

$$X_L = \omega L = 2\pi f L \tag{4.2}$$

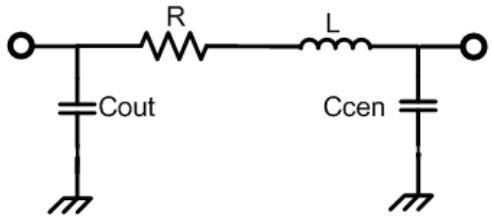

Figure 4.10: Equivalent model for TriQuint HBT spiral inductor

4.3.2 Measurements and Simulations of Spiral Inductors

In order to predict the behavior of spiral inductor some measurements of different spiral inductors have been carried out using a probe-station in the microwave lab. The probe station is connected to a network analyzer in order to display the S-parameters. Pictures of the probe station can be seen in Figure 4.11. The right picture shows the whole probe station with microscope, whilst the left pictures displays the probe needles that are connected to the circuit pads for measuring. Before doing the measurements the measuring setup was calibrated to an open line, shorted line and matched load. The chip that was measured can be seen in Figure 4.12. The numbered circuits represent the measured inductors.

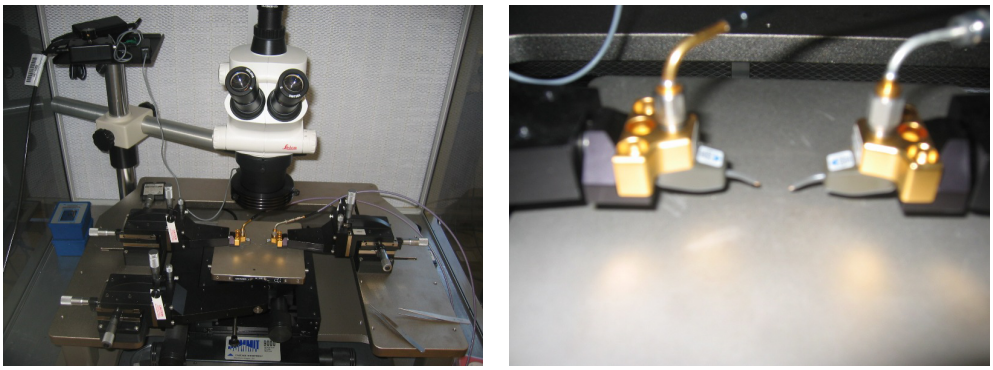

Figure 4.11: Probe station for measuring MMIC circuits.

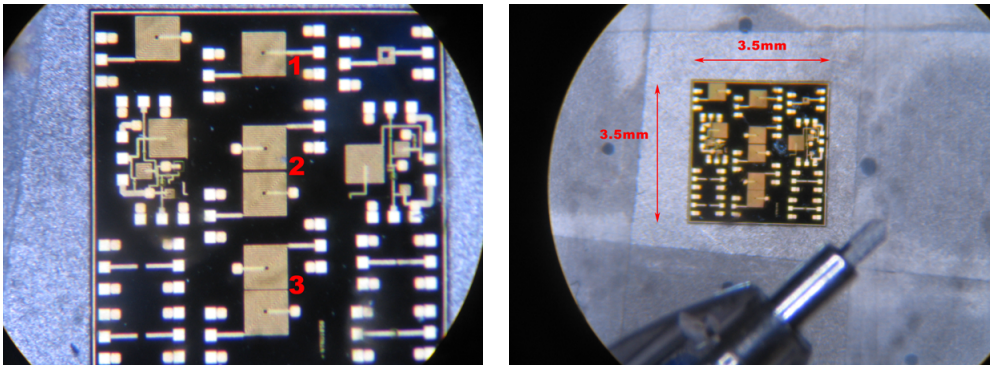

Figure 4.12: Chip through microscope: (left) measured inductor structures; (right) chip compared with 0.5mm pencil tip.

The different inductor circuits are described in the list below. Where the parameters are as follows: conductor width (w), conductor spacing (s), number of quarter turns (n), inductor width (l1), inductor height (l2), underpass width (underWid) and spacing between inductors (s_i).

1. **Single inductor:** metal1 and metal2, w=10 μm, s=10 μm, n=38, l1=400μm, l2=400μm, underWid=20 μm. **Structure:** connected to metal2 transmission lines (30μm x 250μm) and probe pads on each side.

2. **Two wide coupled inductors** metal1 and metal2, w=10 μm, s=10 μm, n=38, l1=400μm, l2=400μm, underWid= 20 μm. **Structure:** the inductors are connected to metal2 transmission lines (30μm x 250μm) and probe pads at input ports of both inductors. The inductors are spaced $s_i = 40\mu m$ apart. At the output ports the inductors are connected to ground vias (90x90μm).

3. **Two tight coupled inductors** metal1 and metal2, w=10 μm, s=10 μm, n=38, l1=400μm, l2=400μm, underWid=20 μm. **Structure:** the inductors are connected to metal2 transmission lines (30μm x 250μm) and probe pads at input ports of both inductors. The inductors are spaced $s_i = 20\mu m$ apart. At the output ports the inductors are connected to ground vias (90x90μm).

Measurements of circuit 1

As listed above the first circuit consists of a single rectangular spiral inductor. The measurements were done as a two-port with the probes connected to pads at each side of the circuit. Each probe consist of three pins, two side pins and one center pin. The side pins are connected two ground through substrate vias. The center probe pin, connected to the center pad, is then used for S-parameter measurements.The measured data is then exported as s2p-file (two port S-parameter

file) to be used in Agilent ADS. In ADS S-parameter simulations are carried out both as a 2-port device and single port device where port 2 is shorted.

The simulation results for a two-port configuration can be seen in Figure 4.13. It can be seen from the S_{21}-plot that there is about 2-11dB loss for the through signal for this inductor. Even though it seems that S_{12}-plot is not present, it is almost overlapping with the S_{21}. This can be seen in the zoomed version of the plot. Therefore it can be said that this inductor structure gives equal response for both ports as input port. The results from the measurement used to compare with EM-simulations and with TriQuint equivalent circuit model to see how they agree with each other.

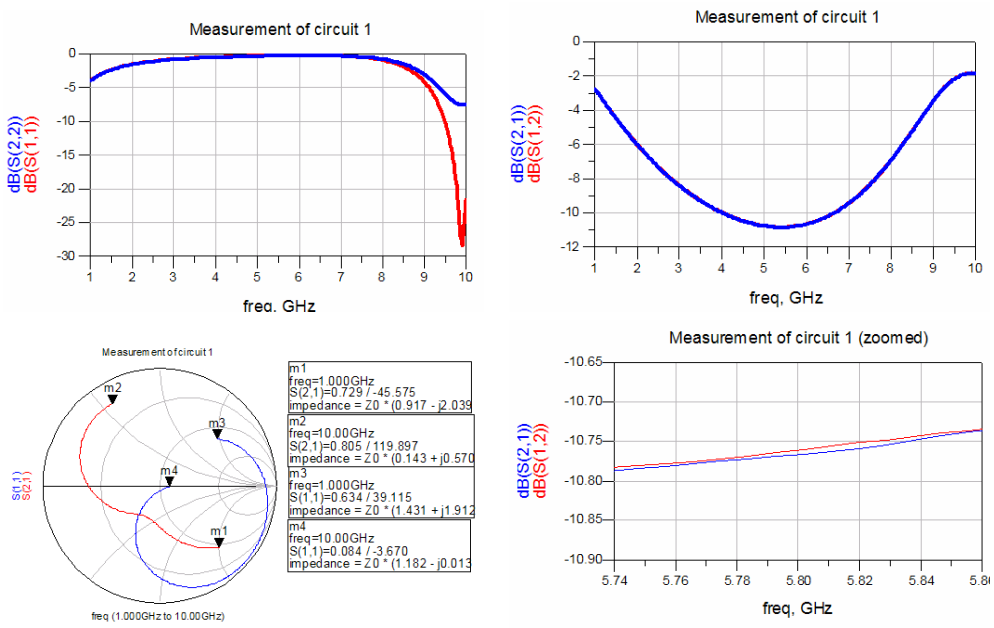

Figure 4.13: Measurements results of circuit 1 from Figure 4.12

Simulation setup for circuit 1 using spiral inductor equivalent model

Since we wish to compare the measurements with the equivalent inductor model some circuit elements have to be added. When measuring the circuit it was connected to lines, pads and vias. All these elements have to be included in order to give basis for comparison. A suggested simulation setup can be seen in Figure 4.14. The metal2 lines are modeled using microstrip lines by defining similar substrate. The pads and vias in the circuit are from the TriQuint HBT3 foundry.

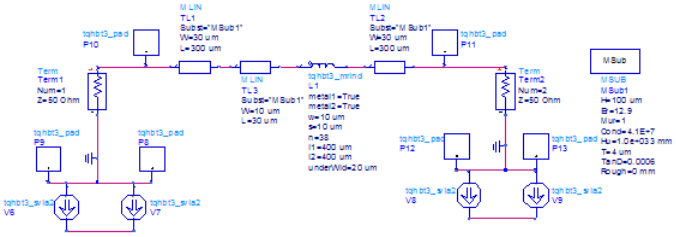

Figure 4.14: Simulation of circuit 1 using equivalent model from TriQuint foundry

EM-simulation setup for circuit 1

The EM-simulations done in Agilent Momentum requires proper setup of the substrate. Unlike the MIM capacitor it is not necessary to use MIM layers. The substrate definition can be seen in Figure 4.15. It illustrates the different dielectrics, metals and vias used for inductor designs, whilst the simulation parameters can be found in Appendix A.

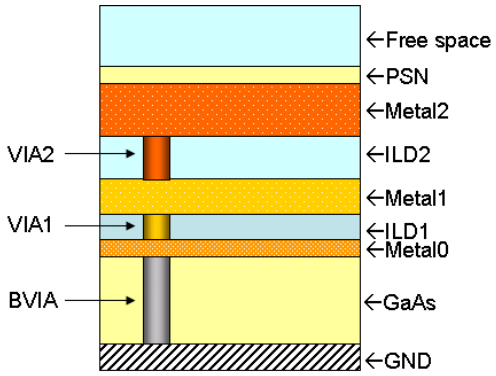

Figure 4.15: Momentum substrate defininsion for non-MIM components

The layout of the spiral inductor in momentum and momentum simulation parameters are set up as in Figure 4.16. Since the spiral inductor has numerous turns and fairly large, a higher mesh density than the MIM capacitor (ch. 4.2.3)is chosen for more accurate field solutions. Additionally since the spiral inductor consists of many long transmission lines, transmission line mesh is set to 4 cells. The transmission line mesh is defined on number of cells that should be in the width of the transmission lines. The simulation results can be seen in the next subsection.

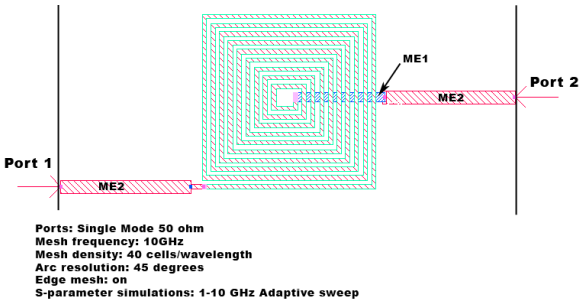

Figure 4.16: Circuit 1 Momentum layout and simulation parameters

Comparison of equivalent circuit, EM-simulations and measured results for circuit 1

Using the setup from above the equivalent circuit, Momentum model and measured results are simulated together for comparison, Figure D.1. The equivalent circuit is connected to terminations 1 (input) & 2 (output), measured data to terminations 3 (input) & 4 (output) and Momentum data to terminations 5 (input) & 6 (output). Circuit 1 is then simulated from 1-10GHz.

The S_{21} simulation (Figure 4.17) shows that the equiv. model and the measured results are quite similar up to 7.5Ghz (difference <0.45dB), whilst the EM-simulated S_{21} is closer to the measured results for frequencies above 7.5GHz (maximum difference <0.5dB). Studying the results from the S_{11}-simulations (Figure 4.18) it is seen that both EM- and equivalent-simulations are in conjunction with the measured results up to 7GHz, but differ far more when the frequency increases. When regarding the phase of S_{21} it is clear that the EM-simulation is to a higher extent in phase with the measured results.

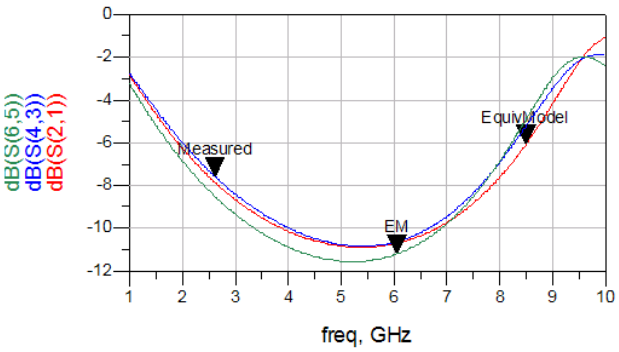

Figure 4.17: S21 comparison for circuit 1. Equivalent model (red); measured results (blue) ; EM-simulated (green)

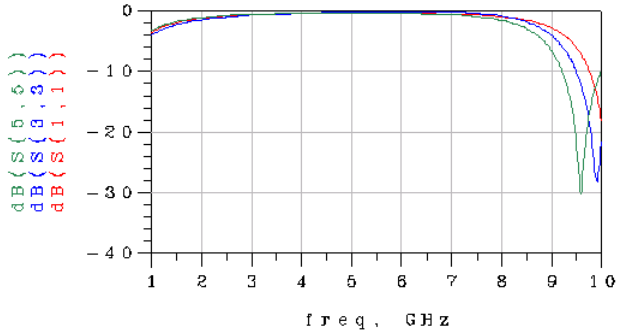

Figure 4.18: S11 comparison for circuit 1. Equivalent model (red); measured results (blue) ; EM-simulated (green)

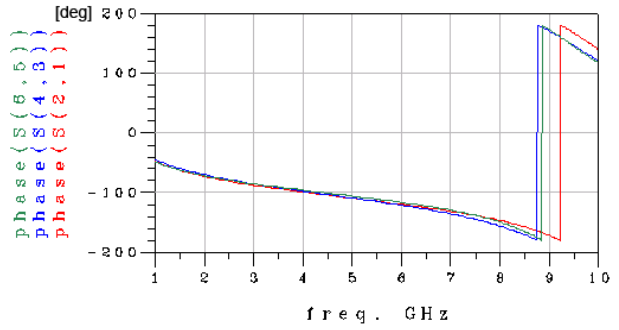

Figure 4.19: S21 phase comparison for circuit 1. Equivalent model (red); measured results (blue) ; EM-simulated (green)

When investigating inductors there are more important measurements to be done such as Self Resonant Frequency (SRF), Q (quality)-factor and inductance. These parameters are often used by manufacturer's to describe inductors. In order to measure these parameters the output ports of our circuits are shorted to give more accurate results. The SRF determines the validity of an inductor in a way that it loses it properties for frequencies above the SRF and introduces a capacitive effect. TriQuint states in its design manual that inductors should preferably not be used above half the SRF. This is something to keep in mind when using inductors in lumped element quadrature hybrids. The self resonant frequency can easily be calculated using formula 4.3, where Z_{11} becomes the input impedance. By plotting the imaginary part of Z_{11} we will find the SRF when the graph turns from positive to negative. From Figure 4.20 it can be seen that EM-simulation gives more accurate SRF at aprroximatly 2.96GHz, whilst the equivalent model differs about 100 MHz. Although the equivalent model differs it can be said to be fairly accurate.

$$SRF: \ Im(Z_{11}) = 0 \tag{4.3}$$

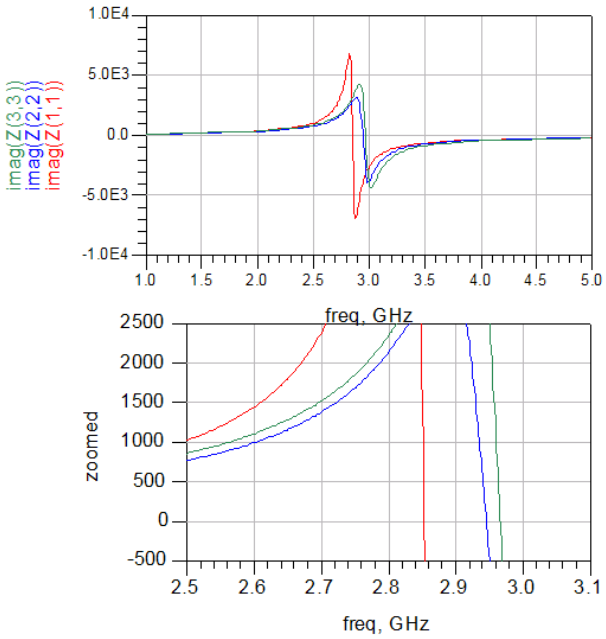

Figure 4.20: SRF comparison for circuit 1. Equivalent model (red); measured results (blue) ; EM-simulated (green)

Since we now know that the SRF is around 3GHz the Q-factor and inductance is simulated below this frequency. Recalling formula 4.2 the inductance

is found as seen in Figure 4.21. Naturally given the SRF from Fig.4.20 we see that the EM-simulation gives a more accurate inductance value. This is given since the inductance is obtained by the reactance as with the SRF.

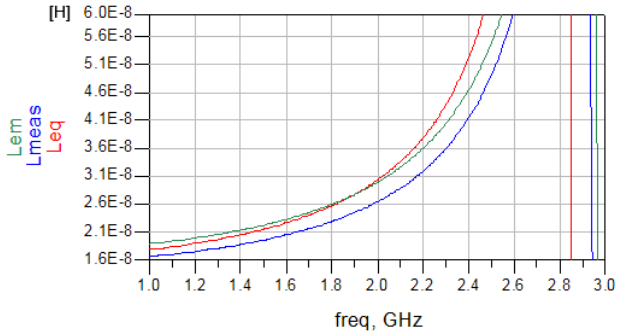

Figure 4.21: Inductance comparison for circuit 1. Equivalent model (red); measured results (blue) ; EM-simulated (green)

Last but not least the quality factor is found using formula 4.4 as described in [21]. By evaluating Fig. 4.22 it is seen that the equivalent model gives too high Q-value than the other simulations. Although the EM-simulation gives higher Q-value it can be said that it is more accurate.

Altogether, with all the simulation results taken into consideration, it can be said that electromagnetic simulations are necessary when designing lumped element hybrids. It gives a more accurate results even though it as well differs from what can be expected from measurements. In order to improve our results, full 3D EM-simulation is preferable when using complex circuits such as with MMICs. Equivalent models can be used to give a fairly good indication of the circuit performance, but should be followed by an EM-simulation for passive circuits to ensure desired response before manufacturing. As said in chapter 3 manufacturing wafers are costly and we can not afford making poor simulations.

$$Q = \frac{Im(Z_{11})}{Re(Z_{11})} \tag{4.4}$$

Coupling between inductors: circuit 2 & 3

When designing compact circuits such as quadrature couplers we might experience coupling between when circuit elements are close to each other. Since most of the current density are on the edge of the coductors in spiral inductors, placing them near each other will result in coupling,[22]. Using equivalent cirucit models in the TriQuint foundry we are not able to simulate coupling effects. Circuits 2 and 3 from Figure 4.12 have been evaluated, where the inductors

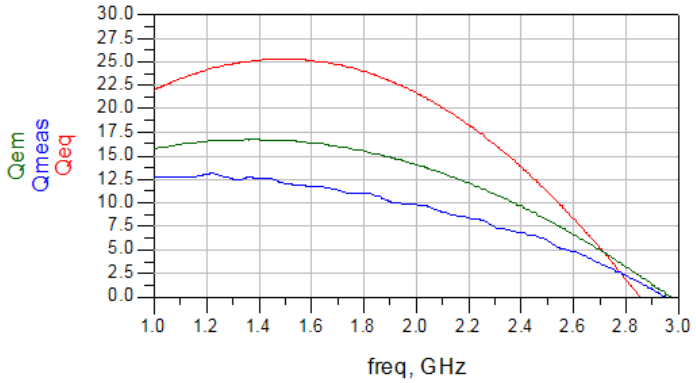

Figure 4.22: Q-factor comparison for circuit 1. Equivalent model (red); measured results (blue) ; EM-simulated (green)

are spaced 40μm and 20 μm apart respectivly. The coupling effects between inductors have been measured using a probe-station and simulated with ADS Momentum. For ADS Momentum the same simulation setup as in Fig. 4.15 and 4.16 are used.

As one can recall from circuit 1 the inductors should not be used above the SRF at 3GHz. The simulation are therefore done between 1-3GHz to maintain the proper inductor response. From Fig. 4.23, the electromagnetic simulations and measured results correspond with maximum of 1dB difference at 3GHz for S_{21}, and almost neglectable difference in S_{11} for the same frequency range. It can be said that the EM-simulations give quite accurate output compared with measured values. The same can be said about results of circuit 3 (Fig. 4.24), which give even better correspondence between EM-simulated and measured results.

When comparing the measured S_{21} of circuits (Fig.4.25) it is obvious that we have a coupling effect between the inductors and that it increases when the inductors are moved closer to each other. In this case when the inductors are moved from 40 μm to 20 μm we increase the coupling by 2.8-3.8 dB. From Figure 4.26, the coupling effect also increases with frequency. Adding up the results it is clear that parasitic coupling occurs if inductors are placed close to each other, this should be avoided when designing lumped element hybrids. Even though the coupling will be minimal at larger distance it still is signifacant and should not be overlooked.

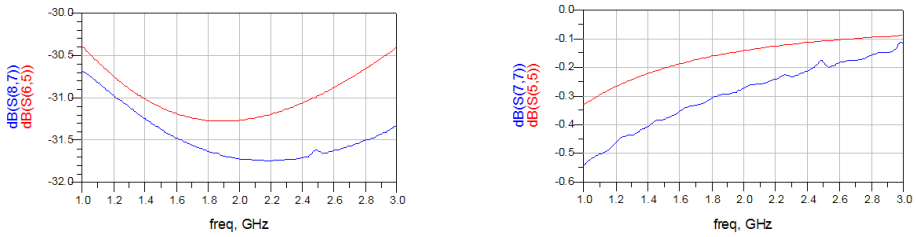

Figure 4.23: Circuit 2: S_{21} (left) and S_{11} (right); EM-simulation (red), Measured (blue)

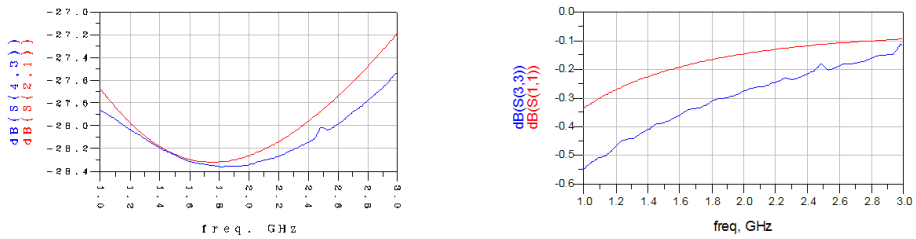

Figure 4.24: Circuit 3: S_{21} (left) and S_{11} (right); EM-simulation (red), Measured (blue)

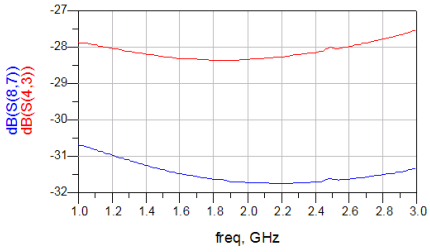

Figure 4.25: Measured S_{21} of circuit 2 (blue) and circuit 3 (red)

4.4 Via-holes

Via holes are used in circuits with multi-layered substrates both for connecting metal layers together and for grounding purposes. From Figure 4.27 we can see

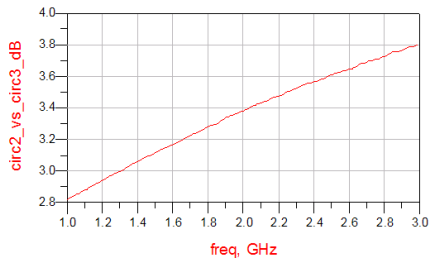

Figure 4.26: Difference in dB between measured S_{21} of circuit 2 and 3

the cross section of the substrate via in the TriQuint HBT process. It consist of all three metal layers (ME0,ME1 and ME2)connected with VIA1 and VIA2. At the bottom layer it is connected to the backside metal wafer plate for grounding the circuit. The equivalent model for the substrate via in the TriQuint design kit consist of an inductor and resistor in series, as can be seen in Figure 4.28. The value of R is given at DC while the L value of 13pH is given at 1GHz.

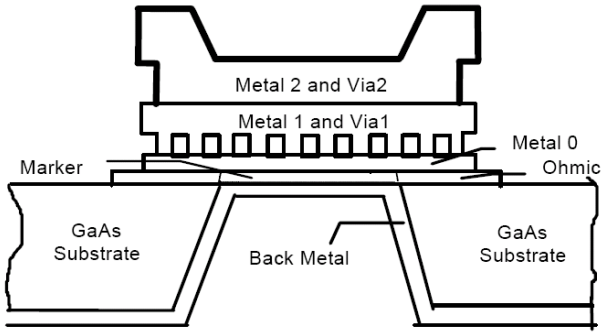

Figure 4.27: Substrate via (SVIA) cross section,[3]

In some lumped element quadrature hybrids, passive components are grounded with substrate vias which will cause extra inductance to be added to the component. A simple simulation of a spiral inductor from 1-10GHz shows how the inductance increases when using substrate vias at output port, Figure 4.29. As seen from the figure to the right, the difference in inductance increases with frequency form 13pH to 31pH. This property can be used to our advantage when designing lumped element quadrature hybrids. If we design circuits where the inductors are grounded with substrate vias, we may use smaller spiral inductors to achieve the desired inductance.

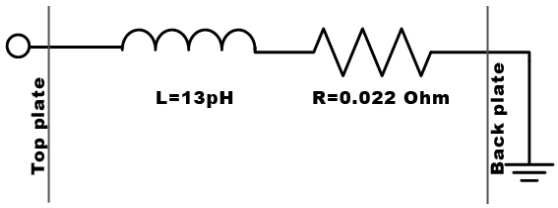

Figure 4.28: TriQuint HBT3 substrate via equivalent model

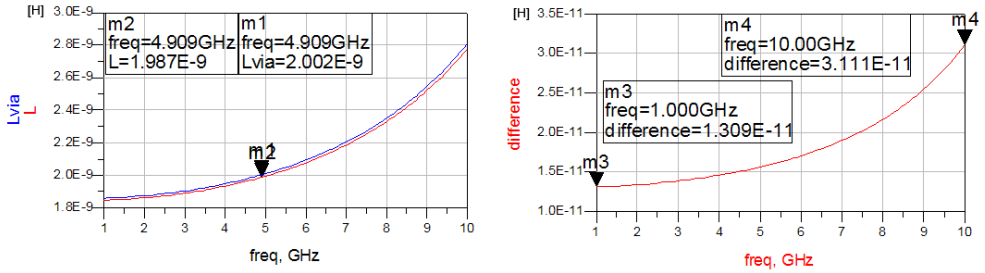

Figure 4.29: Left: L of inductor withouth SVIA (red) and with SVIA (blue) ; Right: Difference in L

Chapter 5

Realization and Simulations of Different Coupler Topologies

In this chapter different coupler topologies are evaluated from literature study to find suitable topologies for MMIC realization. The couplers has to maintain requirements stated in section 1.3. For the sake of common practice the center frequency 5.8GHz is used. This frequency is in the ISM band often used wireless systems. In some cases arbitrary frequencies in the desired frequency range is presented. Matlab-codes for some topologies are written so that design parameters easily can be changed for different frequencies.

5.1 Branch-Line Coupler

5.1.1 Conventional Branch-Line Coupler using $\lambda/4$-Transmission Lines

The branch-line coupler discussed in section 2.4 is the simplest form of 3dB quadrature hybrids. Calculating the line impedances from equations 2.11 and 2.12, or by using matlab code in Appendix B.1, we obtain line impedances of $Z_{01} = 35\Omega$ and $Z_{02} = 50\Omega$. The characteristic impedance (Z_0) is set to 50Ω and coupling factor (C) to 3dB. Calculation of the transmission line lengths for a branch-line coupler is done in ADS LineCalc (Figure 5.1), given the line impedances Z_{01} and Z_{02}. The substrate definition is set using values from Appendix A and frequency to 10GHz, which will result in the shortest $\lambda/4$-lines in our case. We observe that the quarter wave lines become too long, accordingly 2540 μm and 2637 μm. Therefore this topology is not suitable for MMIC technology as it would result in a high chip cost.

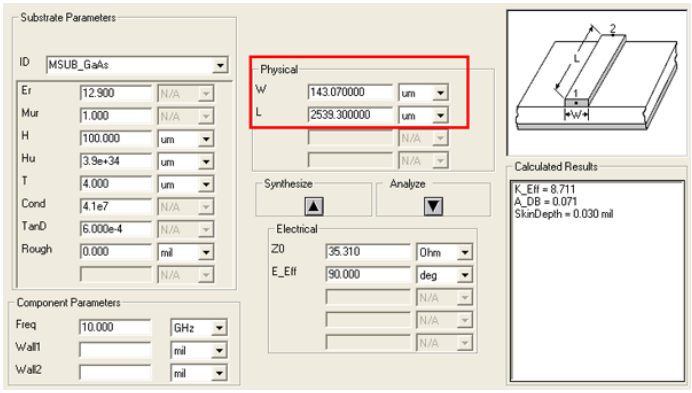

Figure 5.1: Length of transmission lines for a branch-line coupler using ADS LineCalc

5.1.2 Improved Branch-Line Coupler

Since the standard branch-line coupler results in lengthy lines an improved version in presented in [7]. The method used in the paper reduces the $\lambda/4$-transmission lines by using equivalent transmission-line structures such as stepped impedance or T-shaped lines, as seen in Figure 5.2. In the figure Z_0, Z_1 and Z_2 are characteristic impedances and θ, θ_1 and θ_2 the electrical lengths of the transmission lines.

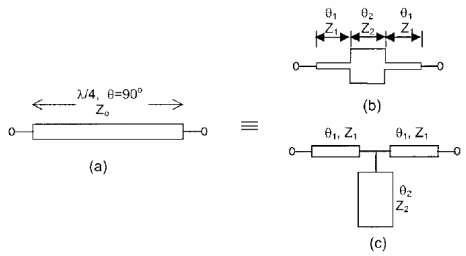

Figure 5.2: (a) $\lambda/4$ transmission line, (b) stepped impedance structure circuit equivalent to $\lambda/4$ line, (c)T-shaped structure circuit equivalent to $\lambda/4$ line; [7]

Using ABCD-matrices,[7], the design equations 5.1 and 5.2 are obtained for the equivalent stepped structure.

$$\theta_1 = \tan^{-1}\sqrt{\frac{K^2 - M^2}{K^2 M^2 - 1}} \tag{5.1}$$

$$\theta_2 = \cos^{-1} \frac{\sqrt{(K^2M^2 - 1)(K^2 - M^2)}}{M(K^2 - 1)} \tag{5.2}$$

where $K = Z_1/Z_2$ and $M = Z_1/Z_0$. The total electrical length is then found by $\theta_T = 2\theta_1 + \theta_2$. In appendix C design curves have been attached for simple for determining M and K. The curves show that the electrical length, for the stepped transmission lines, decreases with increasing the value of K. The equations for the T-shaped configuration follows, given from [7], are given in equations 5.3 and 5.4. In the case of T-shaped configuration the total electric length is $\theta_T = 2\theta_1$. Matlab codes for both configurations are applied in Appendix B, gives room for easy trial-and-error approach of finding suitable K and M.

$$\tan\theta_1 = \frac{1}{M} \tag{5.3}$$

$$\tan\theta_2 = \frac{1}{K}(\cot\theta_1 - \tan\theta_1) \tag{5.4}$$

From table C.1 we see that transmission lines for 5.8GHz become to long, therefore coupler with center frequency at 10GHz is designed. In the design manual [3] it is said that the minimum requirement for metal2 line with is $5\mu m$. From chapter 5.1 we obtained $Z_{01} = 35\Omega$ and $Z_{02} = 50\Omega$.

Looking up in the table of the transmission lines for a $5\mu m$ line width, we obtain $M = Z_1/Z_{02} = 100.3/50 \approx 2$ for the vertical line and $M = Z_1/Z_{01} = 100.3/35 \approx 2.87$ for the horisontal line. Then by using Figures C.1 and C.2 it seen that the T-configuration gives the shortest length lines. The stepped configuration gives $\theta_T \approx 60^\circ$ at the best, whilst using 5.3 we obtain $\theta_T = 2\theta_1 = 53.13^\circ$. The minimum value for K, given that we want a symmetrical structure and the lines not to cross, is set to K=3. the impedance of the T-stub in the vertical line then becomes $Z_2 = Z_1/3 \approx 33.4\Omega$ and we obtain $\theta_T \approx 26.56$.

For the horisontal line we use $M = 2.86 \approx 3$ for the stepped configuration. For K=4 to 6 we obtain total electrical length of 70.3° to 59.4° respectively. K=6 is chosen since it gives the shortest line. It is possible to choose higher K which will result in lower impedance lines that become too large so that we might get undesirable coupling between the lines. Z_2 will then result in a impedance of 16.7Ω, and we have $\theta_1 = 16.1^\circ$ and $\theta_2 = 27.2^\circ$. The final design parameters are given in table 5.1.2. By using ADS LineCalc the transmission lines are obtained as can be seen in Figure 5.3.

A schematic simulation in ADS was carried out with microstrip lines using GaAs as substrate and Metal2 as conducting transmission line. As can be seen from Figure D.2 the through port gives quite satisfying results with 3.1dB power division at 10 GHz, while the coupling is $\approx$ 4.6dB at 10GHz. The circuit has

Transm. line	Config.	$Z_1(\Omega)$	$Z_2(\Omega)$	$\theta_1(^\circ)$	$\theta_2(^\circ)$	$\theta_T(^\circ)$
vertical	T	100.3	33.4	26.56	26.56	53.1
horistontal	stepped	100.3	16.7	16.1	27.2	59.4

Table 5.1: Design parameters for improved branch-line @ 10GHz

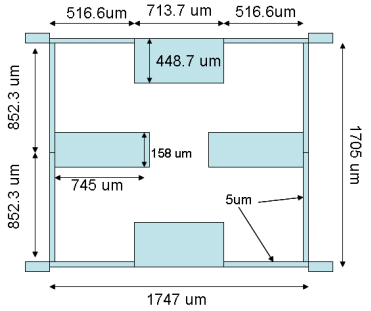

Figure 5.3: Layout of the improved branch-line coupler @ 10GHz

good broadband isolation and return loss under -13dB in the frequency range 9-11.15GHz. The phase balance between the output ports also give fairly good results, $90^\circ \pm 5^\circ$ in the frequency range 8.9-12.8GHz. Generally it can be said that there are two characteristics that do not satisfy our design, namely the output of the coupling port and the bandwidth of our design. After optimization (Fig. 5.4) the coupling is improved but still both power division and bandwidth maintain unsatisfactory. It is also seen that the size of the circuit increases, but still the sides remain approximately 700-800 μm shorter than the conventional branch-line coupler from previous subsection.

It can be said that the improved branch-line coupler design has few advantages compared with other coupler designs. This design method we reduce the size compared with the traditional branch-line coupler, even though the chip size is still fairly large for MMIC applications at frequencies below 10GHz. Even though chip cost will be high because of the size, it only makes use of transmission lines which are cheap to manufacture.

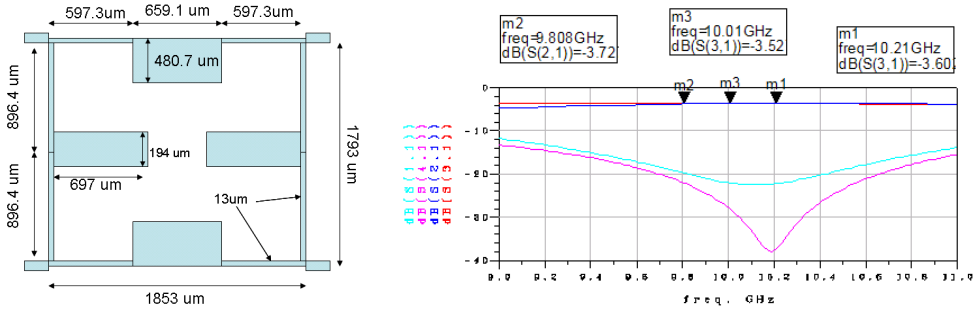

Figure 5.4: Optimized circuit(left) and results (right) for improved branch-line coupler

5.1.3 Improved Branch-Line Coupler with Lumped-Distributed Elements

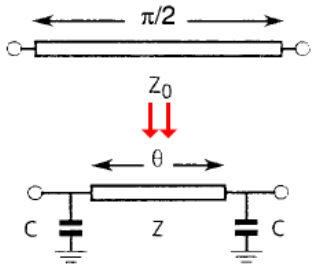

Figure 5.5: Size reduction transformation of a $\lambda/4$-line by introducing shorted capacitors

The coupler designed in previous subsection proved to have somewhat poor coupling and bandwidth. The size was also considerably large. These parameters can be further improved by combining the method above with the method suggested by [23]. The method described in the paper introduces capacitors at the end of the lines in order to shorten the electrical length of the lines, hence reduce the length of the transmission lines, as can be seen in Figure 5.5. The equations for calculating the parameters of the equivalent line with shorted capacitors can be obtained by comparing the admittance matrices of the two equivalent circuits in Fig. 5.5. For the 90° branch-line with characteristic impedance Z, we obtain equations 5.5, 5.6 and 5.7.

$$\theta_1 = sin^{-1}y \tag{5.5}$$

$$\theta_2 = sin^{-1}\frac{y}{\sqrt{2}} \tag{5.6}$$

$$C = \frac{1}{\omega Z_0}(\sqrt{1-y^2} + \sqrt{2-y^2}) \tag{5.7}$$

where θ_1 is the electrical length of vertical line, θ_2 the electrical length of horisontal line, ω the angular center frequency, Z_0 the characteristic impedance, C the capacitance and $y = Z_0/Z$. Which in our case will result in $\theta_1 = 44.5°$, $\theta_2 = 29.6°$ and C =0.8pF. Ideally this method should be applied before using the method in the previous subsection. Since we already have changed the impedances of lines a detour has been taken. In all simplicity the shunt capacitors can be added to the circuit and optimized using Agilent ADS using all the parameters of the circuit. From Figure 5.6(a) it is seen that the dimensions of the circuit has decreased further. The circuit area has decreased 42% from the distributed circuit in Fig. 5.4 and 71% from the convensional branch-line coupler. The circuit has been optimized using 0.44pF TriQuint MIM-capacitor in shunt $90\mu m$ substrate via. From section 4.2 it is seen that the MIM-capacitor gives quite similar results to the circuit model in the foundry. Therefore one can assume that an EM-simulation will result in quite similar results. The through and coupled response, Fig. 5.6(b), displays a power split of 3.3dB +0.2 in the frequency range 9.5-10.6GHz. The coupled port is showing flat response over a wide bandwith, whilst the through port gives a narrower bandwidth but better coupling at the center frequency. The coupler isolation and return loss also gives quite satisfying response. The coupler isolation is infact below -15dB for a 2GHz bandwidth and approximatly -40dB at center frequency,Fig.5.6(c). The circuit also maintains a stable $85°+5°$ phase balance from 8.5 to 11.35GHz. The main drawback of the lumped-distributed branch-line coupler is the bandwidth of the through port. In order to widen the bandwith it is possible to make a multi-section coupler, but it will conclude in a quite large circuit for MMIC realization.

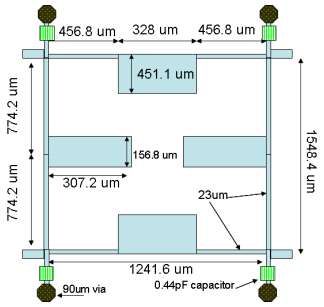

(a) Layout

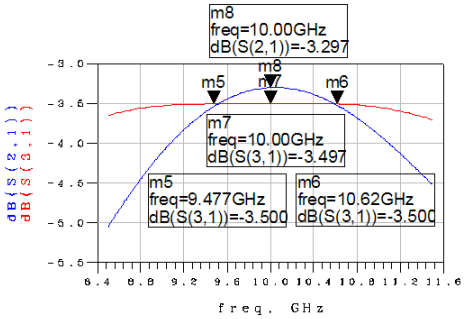

(b) Through(S_{21}) and coupled (S_{31}) results

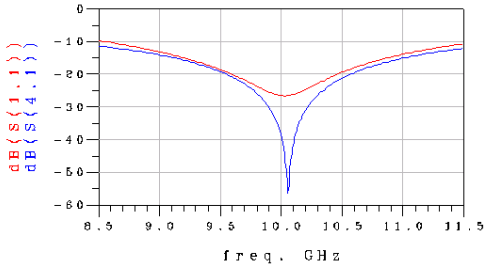

(c) Return loss(S_{11}) and isolation (S_{41}) results

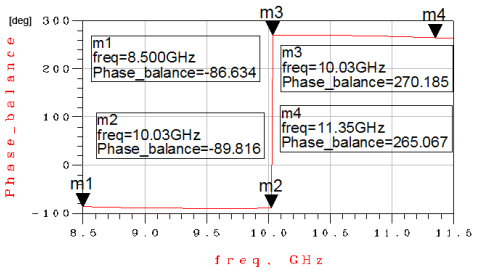

(d) Phase balance

Figure 5.6: Results for the lumped-distributed branch-line coupler

5.2 Lumped Element Quadrature Hybrids

Lumped Elements Quadrature Hybrids are often preferred over distributed couplers since they do not rely on quarter-wavelength lines. The only problem we may face when using lumped elements in MMIC, opposite of distributed, is that the lumped components often give loss and non-linear behavior due to parasitics that occur to the components within the substrate, as discussed in chapter 4.

5.2.1 Topology 1 - Shunt Inductor Design

The topology presented here is based on the paper

> A MMIC lumped element directional coupler with arbitrary characteristic impedance and its application [8].

Unlike most configuration this topology takes the input and output characteristic impedance into consideration. In many systems, such as balanced amplifiers, it may preferable to design the coupler for other impedances than 50Ω to give better matching. Figure 5.7 displays the suggested topology with shunted inductors. If the characteristic impedance at input (Z_1) and output (Z_2) are equal the circuit will remain symmetric.

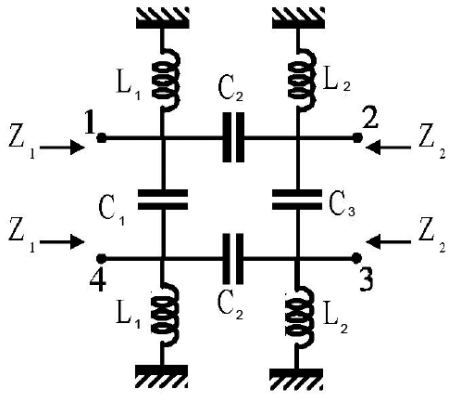

Figure 5.7: Lumped Element Quadrature Hybrid proposed by [8]

The equations for calculating component parameters are derived by using equivalent Y-matrices between the conventional directional coupler and two coupled π-LC circuits. Derivation of the matrices are found in the paper. The systems of equations is given below, where the parameter n is the ratio between input and output characteristic impedance and Z the mean value. ω_0 in this case is the angular center frequency which the coupler will operate at. The equations are also implemented in Matlab for easy calculations, see appendix.

$$n = \frac{Z_1}{Z_2} \tag{5.8}$$

$$Z = \sqrt{Z_1 Z_2} \tag{5.9}$$

$$C_1 = \frac{\sqrt{n}}{\omega_0 Z} \tag{5.10}$$

$$C_2 = \frac{\sqrt{2}}{\omega_0 Z} \tag{5.11}$$

$$C_3 = \frac{1}{\omega_0 Z \sqrt{n}} \tag{5.12}$$

$$L_1 = L_2 = \frac{Z}{\omega_0(\sqrt{2} + \sqrt{n})} \tag{5.13}$$

Implementation

For this coupler input and output impedances are chosen to be 50Ω and center frequency to 5.8GHz. The calculated parameters using equations 5.8-5.13 are given in Table 5.2.

Z_1	Z_2	n	Frequency	C_1	C_2	C_3	L_1	L_2
50Ω	50Ω	1	5.8 GHz	0.549 pF	0.776 pF	0.549 pF	0.568 nH	0.568 nH

Table 5.2: Design parameters for a lumped element quadrature hybrid using topology 1

When looking at Table 5.2 we notice that the values for the inductors are quite descent and will result in compact spiral inductors. The circuit is first simulated using ideal lumped components giving the results in Figure 5.8.The results concur well with desired performance from the given equations. Equal power split is obtained with good isolation at center frequency. The phase balance also is whit in the quadrature property with maximum deviation of 5° for a 28% bandwidth.

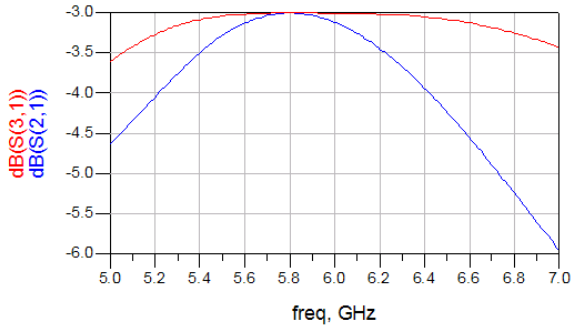

(a) Through(S_{21}) and coupled (S_{31}) results

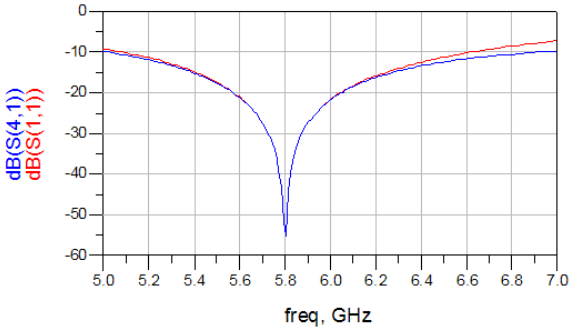

(b) Return loss(S_{11}) and isolation (S_{41}) results

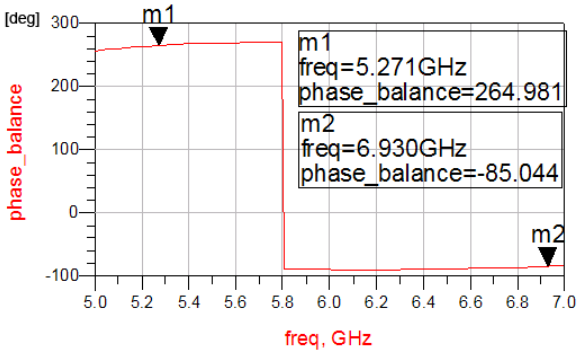

(c) Return loss(S_{11}) and isolation (S_{41}) results

Figure 5.8: Results for the lumped element quadrature hybrid using topology 1 and ideal components

Although, when we use ideal components we are using lossless circuit elements, which is not the case in real life. Therefore we need to replace these with the TriQuint lumped element models. This is done 2 steps. First by adding the MIM-capacitors [tqhbt3_cap] and the substrate vias [tqhbt3_svia] and optimizing the circuit. Then by adding the spiral inductors in the next step. The optimization after the first step is done so that we achieve a coupling of 3dB± 0.5dB. This is necessary since we know from Chapter 4 that the capacitors will be non-linear and that the Vias will add a shunt inductance to the circuit. The results after this step is seen in Figure 5.9. As can be seen from the results the coupled response is flat over a large bandwidth. The through port gives a 3±0.5dB bandwidth of 19%. The isolation has shifted in frequency, but still giving good response. The lumped component parameters after this step is given in Table 5.3, not varying much from the ideal circuit.

C_1	C_2	C_3	L_1	L_2
0.54 pF	0.8 pF	0.54 pF	0.57 nH	0.57 nH

Table 5.3: Design parameters for a lumped element quadrature hybrid using topology 1 with TriQuint MIM-capacitors and substrate vias

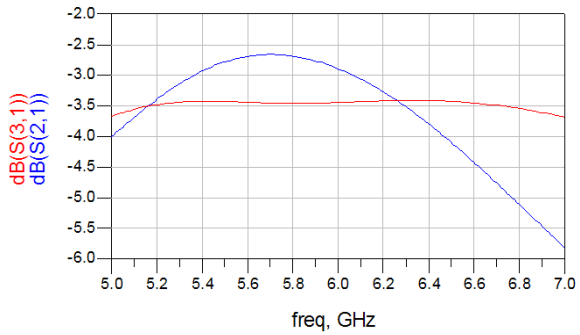

(a) Through(S_{21}) and coupled (S_{31}) results

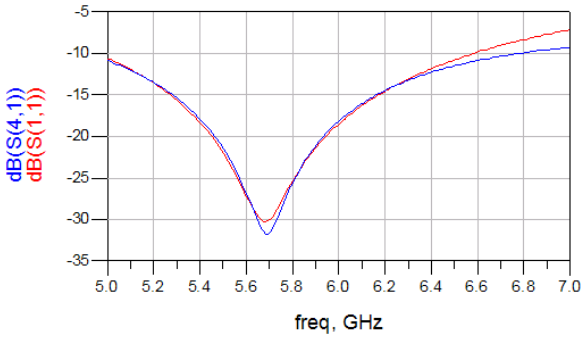

(b) Return loss(S_{11}) and isolation (S_{41}) results

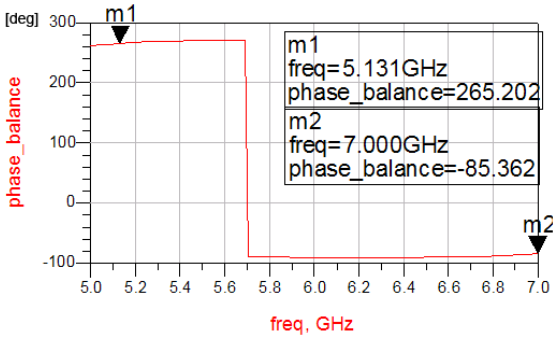

(c) Return loss(S_{11}) and isolation (S_{41}) results

Figure 5.9: Results [Step 1] for the lumped element quadrature hybrid using topology 1. With TriQuint MIM-capacitors and substrate vias and ideal inductors.

Adding the spiral inductors in next step is not intuitive. The inductors has to be designed by varying the inductor parameters without violating the design rules in the design manual. Having these constraints we need to design the inductor by varying its size, conductor widths, number of turns and spacing. Because of the design rule constraints and configuration of the inductor model in ADS, optimization is not possible in a simple manner. Therefore we need to use different trials in order to achieve desired response by tuning. After multiple trials the best performance was achieved with the parameters in Table 5.4, with inductor parameters the same as in section 4.3. The inductance of the spiral inductor is then simulated to be $\approx$ 0.525nH. The size of the two capacitors c1 and c2 will in this case become 23.5x23.5 μm and 27.6x27.6 μm, respectively.

Cap.	C_1	C_2	C_3	Ind.	w	s	n	l1	l2	uw
–	0.58 pF	0.82 pF	0.58 pF	—	$6\mu m$	$7\mu m$	7	$110\mu m$	$110\mu m$	$18\mu m$

Table 5.4: Design parameters for a lumped element quadrature hybrid using topology 1 with TriQuint lumped elements

As seen from the simulation results (Fig. 5.10), the spiral inductors introduce a significant amount of loss to the circuit. The S_{21} and S_{31} drops to just above 4dB power split. The other results on the other hand are satisfactory with good isolation and phase balance. In can be concluded from the results that large amount of shunt inductors is not preffered in lumped element coupler design, since it will introduce unwanted loss. Nevertheless with this topology a notable size reduction have been achieved, since both capacitors and inductors are quite small in size.

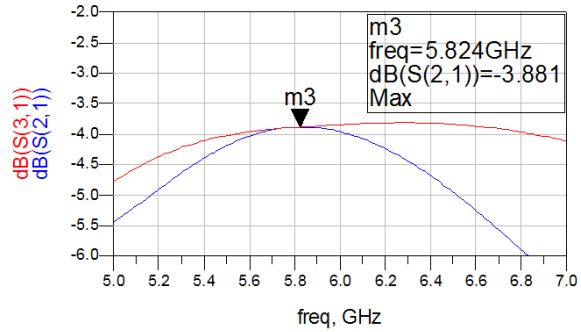

(a) Through(S_{21}) and coupled (S_{31}) results

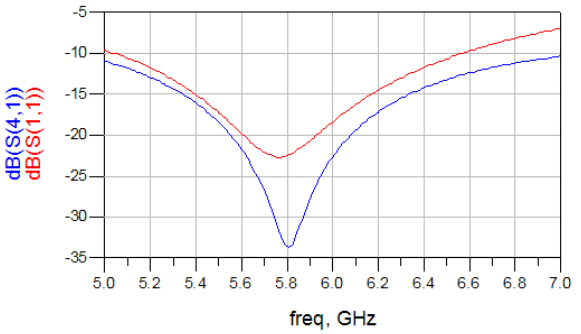

(b) Return loss(S_{11}) and isolation (S_{41}) results

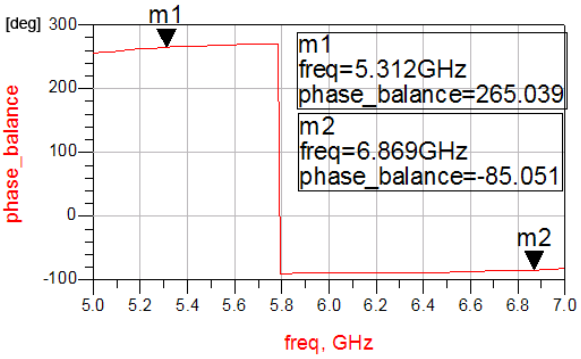

(c) Return loss(S_{11}) and isolation (S_{41}) results

Figure 5.10: Results [Step 2] for the lumped element quadrature hybrid using topology 1 with TriQuint lumped elements

5.2.2 Topology 2 - Two-Inductor Design

From previous topology we observed that the spiral inductors introduced losses that degraded the system performance. Therefore we wish to employ as few inductors elements as possible. The topology used in this section is based on theory from the paper

> Analysis and design of lumped- and lumped-distributed-element directional couplers for MIC and MMIC applications [9].

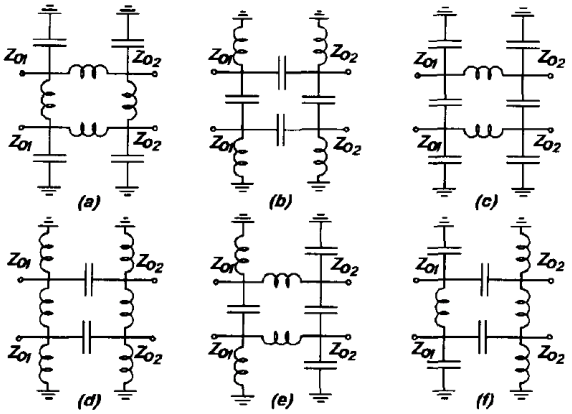

Figure 5.11: Lumped element quadrature hybrid topologies presented by Vogel [9]

The paper presents 6 different coupler topologies as seen in Figure 5.11. The previous topology was based on Fig. 5.11 (b) and used four shunt inductors. In order reduce the number of spiral inductors, hence reduce parasitic losses, we use the topology in Fig. 5.11 (c). From equation systems in the paper the lumped elements can be expressed as:

$$C_1 = \frac{1}{\omega_0 Z_0} \tag{5.14}$$

$$L_1 = \frac{Z_0}{\omega_0 \sqrt{2}} \tag{5.15}$$

$$C_2 = \frac{1}{\omega_0^2 L_1} - C_1 \tag{5.16}$$

Where C1 is the branch capacitors, L1 vertical branch inductors and C2 the shunt capacitors. The same steps as in previous section are carried out. The results of the equations and optimized results with TriQuint lumped elements are shown in Table 5.5. The results from this topology (Fig.5.12)shows that it does not give broadband performance because of the uneven response of the coupled

and through port. As before the the isolation, phase balance and return loss remains satisfactory. The coupler gives a 3.45±0.4 dB over 250 MHz frequency band which only corresponds to 4.5% bandwidth. Therefore this topology is dismissed as a possible quadrature coupler for our purpose.

In the paper a simulation of the circuit in 5.11 (a) is completed using GaAs giving similar results to topology 1 in previous section. Therefore a derivation and simulation of that topology is not done in this thesis.

–	C1	C2	L1
ideal	0.549 pF	0.227 pF	0.97 nH
opt	0.59 pF	0.21 pF	0.92 nH

Table 5.5: Design parameters for a lumped element quadrature hybrid using topology 2 with TriQuint lumped elements

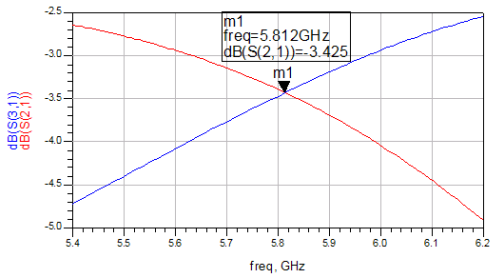

(a) Through(S_{21}) and coupled (S_{31}) results

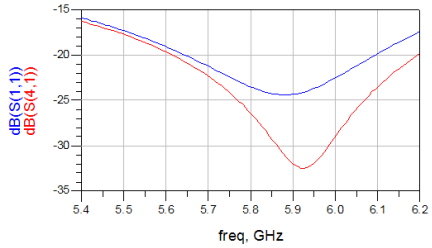

(b) Return loss(S_{11}) and isolation (S_{41}) results

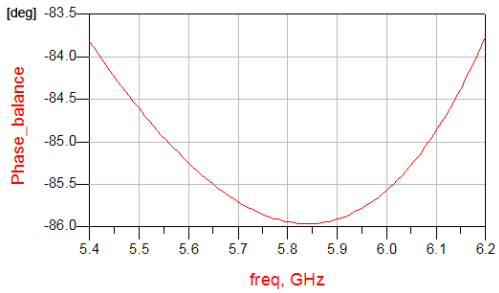

(c) Return loss(S_{11}) and isolation (S_{41}) results

Figure 5.12: Results for the lumped element quadrature hybrid using topology 2 with TriQuint lumped elements.

5.2.3 Topology 3 - Wide-Band Design

If wide-band performance is to be achieved in coupler design it is necessary to introduce couplers consisting of multiple sections of individual couplers. A method for designing wide-band couplers is presented by the paper

> Design of a Wide-Band Lumped-Element 3-dB Quadrature Coupler, [10].

The method used in the paper is based on analysis from [9]. The paper proposes a two-section coupler design using lumped elements as seen in Figure 5.13. The analysis results in two sets of equations that can be used to calculate the element values of Figure 5.13. The values are obtained by equation sets:

$$C_s = \frac{\sqrt{2}}{\omega_C Z_0},\ L_p = \frac{Z_0}{\sqrt{2}\omega_C},\ and\ C_m = \frac{1}{Z_0 2\omega_c} \tag{5.17}$$

$$C_s = \frac{\sqrt{2}}{\omega_C Z_0},\ L_p = \frac{Z_0}{(\sqrt{2}+1)\omega_C},\ and\ C_m = \frac{1}{Z_0 2\omega_c} \tag{5.18}$$

where ω_c is the angular center frequency and Z_0 the input/output impedance.

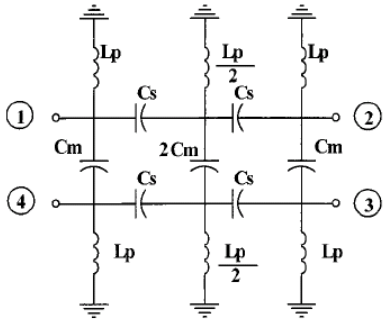

Figure 5.13: Two-section 3-dB quadrature coupler consisting of lumped elements, [10]

Implementation

As before, a quadrature hybrid is implemented using 5.8GHz as center frequency (f_c) and port impedance (Z_0) equal to 50Ω. The element values for the two equation sets 5.17 and 5.18 are given in Table 5.6. The results from S-parameter simulation in ADS using both equation sets are given in Figure 5.14.

From the simulation results it is noticeable that the two equations result in different properties for the coupler. It is seen that both simulations result in much wider bandwidth than the previous topologies.

Equation	C_s [pF]	C_m [pF]	$2C_m$ [pF]	L_p [nH]	$L_p/2$ [nH]
5.17	0.7761	0.2744	0.5488	0.9702	0.4851
5.18	0.7761	0.2744	0.5488	0.5683	0.2842

Table 5.6: Lumped element values for the wide-band quadrature hybrid

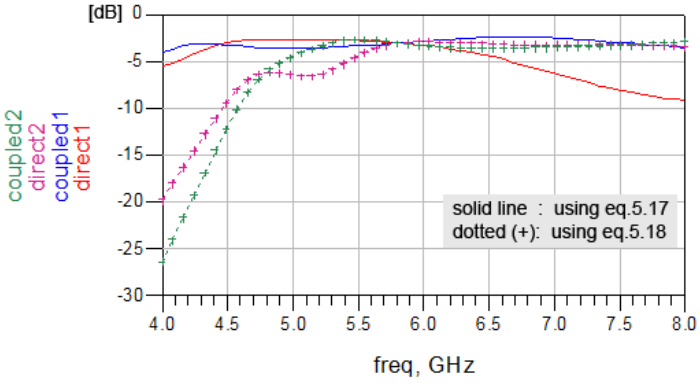

(a) Through(S_{21}) and coupled (S_{31}) results

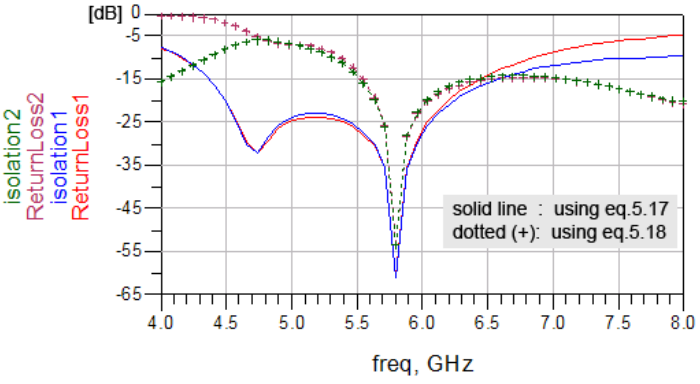

(b) Return loss(S_{11}) and isolation (S_{41}) results

Figure 5.14: Results for the lumped element quadrature hybrid using topology 3 with ideal components.

Using equation 5.17 we achieve approximately a 30% fractional bandwidth for a 0.55 dB amplitude balance. From Figure 5.14(a) it is seen that the direct through port (S_{21}) decreases considerably 6.2GHz, while the coupled port (S_{31}) maintains acceptable performance for larger frequencies. The isolation and return loss, Fig. 5.14(b), from the same equation set also gives values below -20dB at the same frequency range.

On the other hand, the simulation results using equation set 5.18 gives a much more flat coupling and directivity response for frequencies above the center frequency. A fractional bandwidth of approximately 40% is achieved using this procedure. Since the flat response is not centered around the center frequency, it is apparent to use a lower center frequency in the equation in order to center the response around the actual desired center frequency. From Figure 5.14(a) we can assume that lowering the center frequency by 1 to 1.2 GHz should give close to equal flat response on both sides of the center frequency. By applying this approach the isolation and return loss has slightly reduced performance compared to the approach when using equation 5.17.

Summed up the first approach will result in good isolation and return loss response, while the second approach will result in flat amplitude balance over a larger frequency band. It can not be said that one approach is better or worse than the other, it is up to the circuit designer to choose which approach that is appropriate for the application which the coupler is to be utilised. For some applications isolation is of importance, while others require broader bandwidth.

Since no isolation requirements are made in chapter 1.3, equation set 5.18 is used for implementation in order to achieve broadband performance. As mentioned before a lower center frequency should be chosen to achieve as even as possible response on both sides of the actual center frequency. In order to design a coupler for 5.8 GHz a center frequency of $f_c = 4.8$ GHz is chosen. Calculation results for element values are displayed in Table 5.7. The simulation results using element values from the table are found in the Appendix [Fig. D.3]. From the results a fractional bandwidth of 35% for a amplitude balance of 3dB$\pm$0.5. As can be seen from Figure D.3(b) the center frequency chosen for the design equations give the best isolation although we achieve -14dB and better isolation over a 2 GHz bandwidth. The phase balance in Figure D.3(c) shows a quite stable quadrature phase over a 2.5 GHz bandwidth.

C_s [pF]	C_m [pF]	$2C_m$ [pF]	L_p [nH]	$L_p/2$ [nH]
0.93783	0.33157	0.66315	0.68671	0.34335

Table 5.7: Lumped element values for wide-band quadrature hybrid operating at 5.8 GHz using equation set 5.18 for f_c =4.8 GHz

In the final stage the ideal components are replaced with TriQuint lumped elements. Then by using tuning tool in ADS the best response solution is found by varying the lumped element values. Unfortunately, the response is again

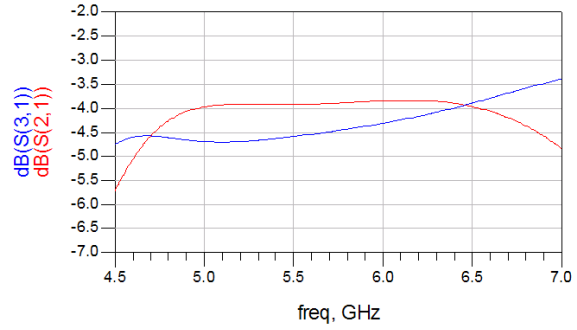

(a) Through(S_{21}) and coupled (S_{31}) results

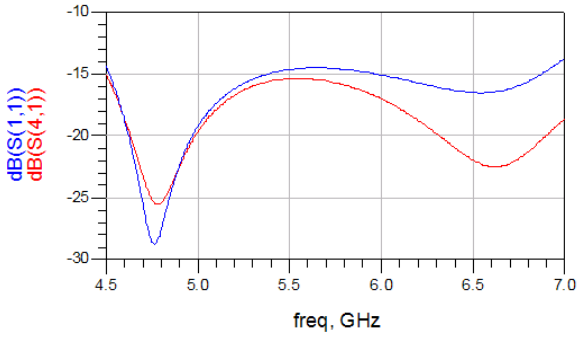

(b) Return loss(S_{11}) and isolation (S_{41}) results

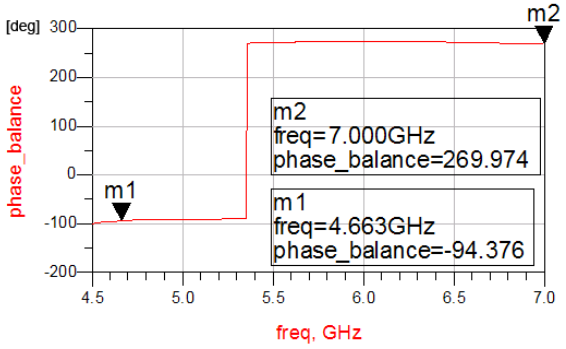

(c) Phase balance

Figure 5.15: Simulation results using wide-band topology and eq. 5.18 with TriQuint lumped elements

marked by the poor performance of the spiral inductors, as seen with previous topologies. The final results can be seen in Figure 5.15. After substituting the ideal with the non-ideal components from TriQuint, the circuit has a loss of about 1.5dB for the coupling and through port performance. This can be seen by comparing 5.15(a) with D.3(a) in the Appendix. Isolation and return loss, as well as the phase balance in Fig. 5.15, display good performance in accordance with the ideal coupler. Also the broadband performance is upheld. Measurements done in paper by Chiang [10] also displays similar performance for 2.4 GHz, so the results obtained in this thesis can be said to relate with measurements from the paper.

5.2.4 Topology 4 - Two Coupled Spiral Inductors

In section 4.3 coupling between inductors were discussed and how it will give parasitic effects. If the coupling effect is strong this effect can be used to our advantage. The paper

A Compact MMIC 90° Coupler for ISM Applications

introduces a new way of using coupled inductors to achieve compact coupler design and better performance. This topology uses the same circuit setup as in section 5.2.2 by making use of concentrical spiral inductors as can be seen in Figure 5.16. The spiral inductor is the key feature to the compact coupler in this topology. Since this topology is quite time consuming and could be a thesis of its own, it is not investigated further here. The method requires a design of own inductor models not present in the foundry. Although, it can be interesting for the reader to investigate this further as part of future work. Using mutual coupled inductors can be done in numerous ways, and not only in the way described in Figure 5.16(b). For example since TriQuint process has different layers, two separate inductors can be designed in Metal2 and Metal1 layers respectively. In order to design this type of coupler numerous EM-simulations of different coupled inductor structures has to be made so that a valid method can be determined. Design graphs should be made by varying number of turns, gap widths and conductor widths. The paper gives a set of equations but these will react differently when using different foundries. In other words the method should be evaluated analytically for the TriQuint foundry by the designer that wishes to investigate the method further.

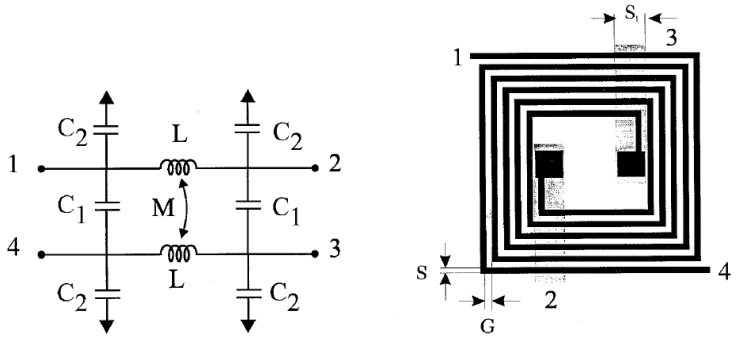

(a) Circuit model (b) MMIC implementation

Figure 5.16: Concentrical spiral inductors, [11]

5.2.5 Lumped Element Quadrature Hybrid Layout

Since desired 3dB coupling was not achived, EM-simulations of a lumped element was omitted. Even though an example layout of a 5.8 GHz coupler using

topology 1 is implemented to show the degree of size reduction achieved by lumped element coupler design. Figure 5.17 displays a suggested coupler layout using same element values as in section 5.2.1. From the figure it can be seen that the chip area has been reduced by 96% compared with conventional transmission line branch-line coupler, that is from 6 697 980 μm^2 to 219 600 μm^2.

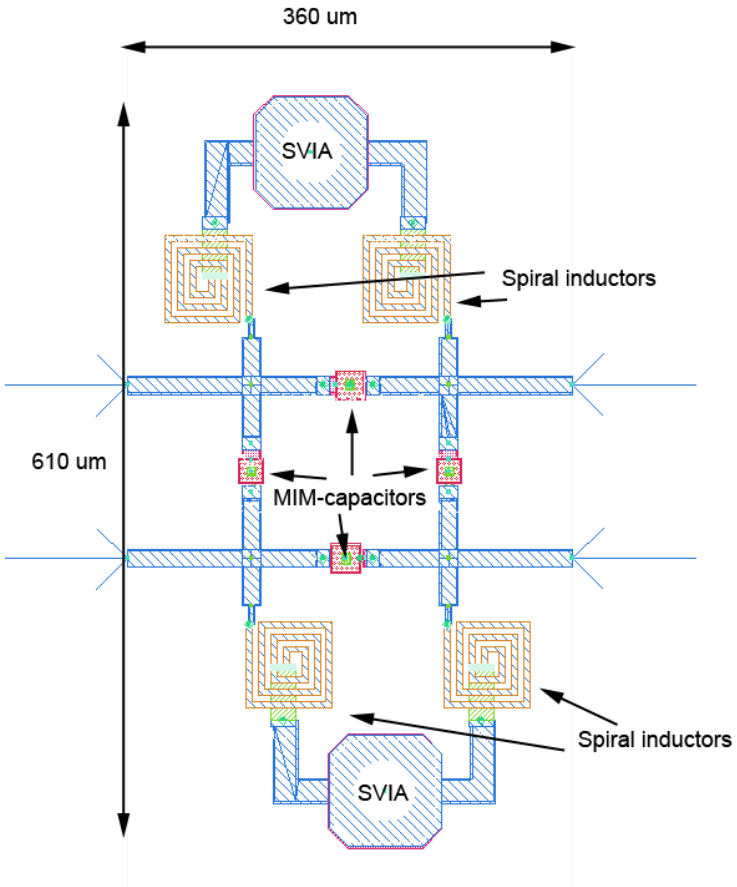

Figure 5.17: 5.8 GHz Quadrature hybrid layout using TriQuint HBT3 lumped elements

Chapter 6

Summary

6.1 Discussion

During this thesis a number of tasks was completed regarding 3 dB quadrature hybrids.

Coupler and MMIC Theory

At first necessary theory regarding basic coupler structures was introduced to show some of the design variations available for design. Different coupler applications were introduced to give the reader insight in the importance of couplers in microwave circuits. Couplers today play an important role in radio systems where dividing and combining are needed.

Further more the MMIC technology has been evaluated to show its advantages and disadvantages of the technology compared with competing products. It was shown that MMIC holds a strong position in miniature microwave circuit design, giving compact high performance circuits at competitive prices if proper layout and precautions are withheld by the designer.

Measurements and Characterization of Passive Components

Measurements of previous produced MMIC circuits were done using a probe station and network analyser. The circuits were manufactured using TriQuint HBT3 process. The measured results were compared with EM-simulations in Momentum and circuit models in Agilent ADS. It has been shown that the MIM-capacitor models in ADS gave quite similar results for circuit simulation and for EM-simulation. Unfortunately capacitor circuits were not available for measurements.

Spiral inductors on the other hand differed slightly from measured results in ADS. Measurements were done using the same spiral inductor and can therefore not be seen as a general solution. Different inductor designs may result in

various deviations from measured results. Even though, the results from the measurements done in this thesis gives the reader a pointer on how spiral inductors react in real life applications compared with simulations done with a CAD program.

Coupling effects between inductors was measured to show how components placed close to each other in a coupler layout might affect the performance and introduce parasitic effects. A microwave circuit designer should be aware of this fact when designing the layout of a MMIC coupler or other circuits.

Via-holes which are often used in MMIC applications were also evaluated showing that gradually increasing inductance was added when substrate vias was employed in the circuit.

Coupler Topologies

Conventional coupler structures using transmission lines is shown to take up large chip space and therefore not suitable for MMIC realization. Different topologies have been proposed to reduce the size of the couplers.

The improved branch-line coupler displayed good coupling and directivity properties with a size reduction of 71% from the conventional branch-line coupler using only transmission lines. The improved branch-line coupler was designed by combining two known methods, namely stepped impedance lines and shunt capacitors. Nevertheless it is concluded that the size would be too large for broadband realization.

Four different topologies were suggested using lumped element TriQuint components. Designs for both narrowband and wide-band were introduced. All the suggested topologies had a similar downgrading factor which was coupling and directivity loss due to the spiral inductors. Apart from this all the topologies had good phase balance, return loss and isolation. A topology using coupled spiral inductors was suggested for future work for the reader. This method requires inductor design and was therefore not pursuit further in this thesis, but is interesting to follow up.

Since spiral inductors are the most space consuming of the passive components in MMIC. All the topologies proposed in this thesis resulted in low inductance values, hence small sized spiral inductors. Generally the use of lumped elements in coupler design reduces the size considerably. In this task inductors were designed by trial and error and therefore not giving optimal solutions. In order to be able to design quadrature hybrids with higher performance, a good modeling procedure for inductors is needed. For future work the designer should attach importance to this problem before designing the coupler.

6.2 Conclusion

Different procedures for designing quadrature hybrids have been presented using TriQuint HBT3 process. Techniques for reducing chip size of couplers have been described. A size reduction of <71% was achieved. Generally great im-

provements regarding size reduction have been achieved. Using methodology described in this thesis it is possible to design quadrature hybrids for different input/output impedance, frequencies and bandwidths.

The results show coupling and directivity of 4± 0.5dB, whilst return loss and isolation of > -20dB was achieved. All topologies resulted in good phase balance of 90° ± 5° over a large bandwidth, giving the circuits the desired quadrature performance. A wide-band topology has been presented to achieve a fractional bandwidth larger than 35%.

Measurements of previous manufactured circuits have been carried out to show how passive circuits correspond with simulations using equivalent models in Agilent ADS and EM-simulations in ADS Momentum. The spiral inductors in the quadrature hybrids were shown to restrain the performance of coupling and directivity and should be investigated further as part of future work.

The designs mentioned in the thesis has been carried out using circuit simulations, EM-simulations and experimental results are omitted since desired coupling and directivity was not achieved using the TriQuint HBT3 process.

6.3 Future work

In order to finalize a quadrature hybrid design many presumption are needed from the designer. The field of coupler design in MMIC requires thorough calculations and knowledge by the designer in order to make a high performance design. Therefore some task for future work is proposed, which was not carried out due to time constraint and lack of resources. Some suggestions for future work are given and commented in the list below:

- Develope a methodology for designing spiral inductors to give low loss when employing the components in quadrature hybrids. Poor inductor performance was shown to be a bottle neck for the overall coupler performance.
- Compare simulations of MIM-capacitors with measured results, since such circuits was not available for measurement for this thesis.
- EM-simulations of a complete coupler design. Because desired circuit performance was not achieved this was not carried out.
- Develope a methodology for designing mutually coupled spiral inductors for use in topology 4.
- Learn and perform design rule checking using Agilent ADS
- Tolerance and sensitivity analysis using Monte Carlo yield simulations in Agilent ADS. Even though manufacturing MMIC circuits are said to be precise, manufacturing errors may arise. Therefore it is necessary to see

how such errors may effect the circuit performance. Packaging may also effect the coupler performance and therefore also evalutated.

- Many different litterature on coupler designs are available from different resources. Only a fraction of these are evaluated in this thesis, and therefore other topologies and techniques should be investigated further in order to find the optimal design.

Bibliography

[1] David Andrews. *Lumped Element Quadrature Hybrids*. Artech House, 2006.

[2] Guillermo Gonzalez. *Microwave Transistor Amplifiers*, pages 327–333. Prentice-Hall, 1997.

[3] TriQuint Semiconductor. TQHBT3 Design Manual. Version 1.7.

[4] TriQuint Semiconductor. Foundry brochure. TriQuint Homepage.

[5] J.Lee, D.Kim, Y.Park, M.Sohn, and K.Seo. DC and RF Characteristics of Advanced MIM Capacitors for MMICs Using Ultra Thin Remote-PECVD Si3N4 Dielectric Layers. *IEEE microwave and guided wave letters*, 1999.

[6] I.D. Robertson. *MMIC Design*. The Institution of Electrical Engineers, 1995.

[7] Abdel Fattah Sheta, Ashraf Mohra, and Samir Mahmoud. A new class of miniature quadrature couplers for MIC and MMIC applications. *Wiley periodicals: Microwave and optical technology letters*, Vol. 34(NO. 3), August 2002.

[8] A.Cidronali, G.Collodi, M.R. Deshpande, N.El-Zein, H.Goronkin, G. Manes, V.Nair, and C.Toccafondi. A MMIC lumped element directional coupler with arbitrary characteristic impedance and its application. *European Microwave Conference*, 2000.

[9] Ryszard W. Vogel. Analysis and design of lumped- and lumped-distributed-elementdirectional couplers for MIC and MMIC applications. *IEEE Trans. on Microwave Theory and Techn.*, 40, 1992.

[10] Yi-Chyun Chiang. Design of a Wide-Band Lumped-Element 3-dB Quadrature Coupler. *IEEE Trans. on Microwave Theory and Techn.*, 49, 2001.

[11] G.F. Avitabile, A. Cidronali, C. Salvador, and M. Speciale. A Compact 90° Coupler for ISM Applications. *IEEE Trans. on Microwave Theory and Techn.*, 1997.

[12] David M. Pozar. *Microwave Engineering*. John Wiley and Sons, 2005.

[13] Peter B. Kenington. *High-Linearity RF Amplifier Design*. Artech House, 2000.

[14] J. Lange. Interdigitated Stripline Quadrature Hybrid. *IEEE Trans. Microwave Theory Tech.*, MTT-17:1150–1151, 1969.

[15] R.M. Osmani. Synthesis of Lange Couplers. *IEEE Trans. Microwave Theory Tech.*, 1981.

[16] Sammy Kayali, George Ponchak, and Roland Shaw. *GaAs MMIC Reliability Assurance Guideline for Space Applications*. JPL Publication, NASA, California Institute of Technology,Pasadena, California, 1996.

[17] Ira Deyhimy. Gallium arsenide joins the giants. *IEEE Spectr.*, 32(2):33–40, 1995.

[18] James M. Moniz. *Is SiGe the future of GaAs for RF Applications?* Gallium Arsenide Integrated Circuit (GaAs IC) Symposium, IEEE, 1997.

[19] Otto Berger; TriQuint Semicond. Inc. GaAs HBT for Power Applications. *IEEE Journal*, sept. 2004.

[20] Agilent Technologies. ADS documentation 2006A. Bundled with Agilent ADS 2006A, 2006.

[21] G.Lihui, Y.Mingbin, C.Zhen, H.Han, and Z.Yi. High Q Multilayer Spiral Inductor on Silicon Chip for 5-6 GHz. *IEEE Electron device letters*, 2002.

[22] Yu Cao, R.A. Groves, X. Huang, N.D. Zamdmer, J.-O. Plouchart, R.A. Wachnik, T.J. King, and C. Hu. Frequency-independent equivalent-circuit model for on-chip spiral inductors. *IEEE Journal of solid-state circuits*, 2003.

[23] T.Hirota, A. Minakawa, and M. Muraguchi. Reduced-Size Branch-Line and Rat-Race Hybrids for Uniplanar MMIC's. *IEEE Trans. on Microwave Theory and Techniques*, Vol. 38, 1990.

Appendix A

TQHBT EM Simulation Parameters

EM Simulator Parameters, no MIM

GDSII	layer	T	Mat.	Cond.	Er	L Tan	Re(Mu)	Im(Mu)
				S / m				
	PSN	0.8	SiNx		6.8	0.0004	1	0
17	ME2	4.0	Gold	4.1e7				
	ILD2	3.2	BCB		2.8	0.0006	1	0
16	VIA2	1.2	Gold	4.1e7				
15	ME1	2.0	Gold	4.1e7				
	ILD1	1.0	BCB		2.8	0.0006	1	0
14	VIA1	0.6	Gold	4.1e7				
9	ME0	0.4	Gold	2.632e7				
	GaAs	100	GaAs		12.9	0.0006	1	0

EM Simulator Parameters, with MIM

	layer	T	Mat.	Cond.	Er	L Tan	Re(Mu)	Im(Mu)
		Um		Sie / m				
	PSN	0.8	SiNx		6.8	0.0004	1	0
17	ME2	4.0	Gold	4.1e7				
	ILD2	3.2	BCB		2.8	0.0006	1	0
16	VIA2	1.2	Gold	4.1e7				
15	ME1	2.0	Gold	4.1e7				
	ILD1	1.0	BCB		2.8	0.0006	1	0
14	VIA1	0.35	Gold	4.1e7				
23	MIM	0.2	Gold	2.632e7				
	CSN	0.05	SiNx		6.8	0.0004	1	0
9	ME0	0.4	Gold	2.632e7				
	GaAs	100	GaAs		12.9	0.0006	1	0

Appendix B

Matlab codes

B.1 Branch-line coupler

```
%calculation of Branch-line coupler
%code by Houman Mohebbi

C=3; %coupling factor in dB
Z0=50; %Characteristic impedance in Ohm

Z01=Z0*sqrt(1-(1/(10^(C/10)))) %impedance of line with impedance Z01

A=Z01/Z0;

Z02 = Z0*(A/sqrt(1-(A^2))) %impedance of line with impedance Z02
```

B.2 Improved Branch-Line with Capacitors

```
%%Improved branch—line coupler with capacitors
%Matlab code by Houman Mohebbi

Z1=35;    %Characteristic impedance of horisontal TL [Ohm]
Z0 = 50;   %input and output impedance [Ohm]
freq0=10e+9; %Center frequency [Hz]

y=Z1/Z0;


w=2*pi*freq0; %angular frequency
theta_1=asin(y)*180/pi % lenght of the vertical line
theta_2=asin(y/sqrt(2))*180/pi % lenght of the horisontal line

C= (1/(w*Z1))*(sqrt(1—y^2)+sqrt(2—y^2))*(10^12) %capacitance on [pF]
```

B.3 Lumped Element Quadrature Hybrid - Topology 1

```
% Equations for lumped element quadrature coupler
% given by "A MMIC lumped element directional coupler with arbitrary
% characteristic impedance and its application"
% code by Houman Mohebbi

%BEGIN:VARIBLES TO SET %

Z1 = 50;  %characteristic impedance at port 1 & 4 (system)
Z2 = 50;  %characteristic impedance at port 2 & 3 (termination)
freq0 = 7.5e+9; %center frequency

%END: VARIBLES TO SET %

w0 = 2*pi*freq0; %angular frequency
n=Z1/Z2; % ratio between system and termination characteristic impedance
Z= sqrt(Z1*Z2); %mean value

c1 = sqrt(n)/(w0*Z) %capacitor C1
c2 = sqrt(2)/(w0*Z) %capacitor C2
c3 = sqrt(1)/(w0*Z*sqrt(n)) %capacitor C3

l1 = Z/(w0*(sqrt(2)+sqrt(n))) %inductor L1
l2 = Z/(w0*(sqrt(2)+sqrt(n))) %inductor L2
```

B.4 Lumped Element Quadrature Hybrid - Topology 2

```
%Coupler topology 2 based on article by R. Vogel
% Matlab code by Houman Mohebbi

Z0 = 50; % port impedance in Ohm
freq=5.8e9; %coupler center frequency

w0=2*pi*freq; %angular center frequency

C1= 1/(w0*Z0) %Capacitor C1
L1 = Z0/(w0*sqrt(2)) % Inductors
C2 = (1/(L1*w0^2))—C1  %Shunt capacitors
```

B.5 Lumped Element Quadrature Hybrid - Topology 3

```
%Design of a Wide-Band Lumped-Element 3-dB Quadrature Coupler
%Matlab-code by Houman Mohebbi

Z0=50; %port impedance in Ohm
freq= 4.8e9; %Center frequency in Hz

w0=2*pi*freq; %angular center frequency

%Using Equation set 5.17
Cs = sqrt(2)/(Z0*w0)
Cm = 1/(2*Z0*w0)
Lp = Z0/(sqrt(2)*w0)

%Using Equation set 5.18
Cs2 = sqrt(2)/(Z0*w0)
Cm2 = 1/(2*Z0*w0)
Lp2 = Z0/((sqrt(2)+1)*w0)
```

Appendix C

Improved Branch-Line Coupler Design Parameters

C.1 Transmission Line Parameters for TriQuint HBT3 Process

W (μm)	Z_c (Ω)	λ (mm) @5.8GHz	λ (mm) @10GHz
5	100.274	19.927	11.5506
6.5	95.99	19.784	11.4674
10	88.522	19.533	11.3213
15	81.03	19.283	11.1757
20	75.47	19.100	11.0687
30	67.38	18.833	10.9125
50	56.86	18.473	10.7020
80	47.06	18.097	10.4813
100	42.47	17.897	10.3632
200	29.07	17.197	9.9520
250	25.23	16.959	9.8120
300	22.33	16.763	9.6969
400	18.19	16.457	9.5169
500	15.38	16.226	9.3811

Table C.1: Transmission line parameters for TriQuint HBT3 process using Metal2

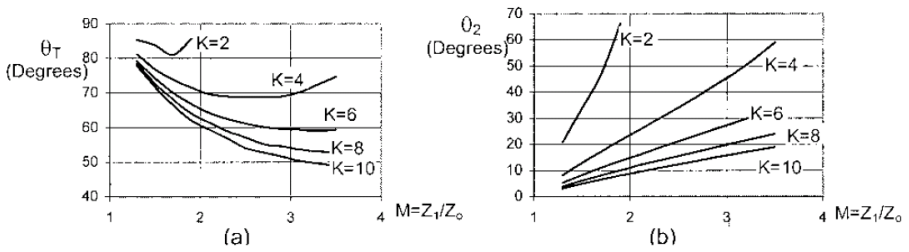

Figure C.1: Design curves for stepped impedance approach; (a) Total electric length θ_T against M for different values of K. (b) electrical length of the midline θ_2 against M for different values of K., [7]

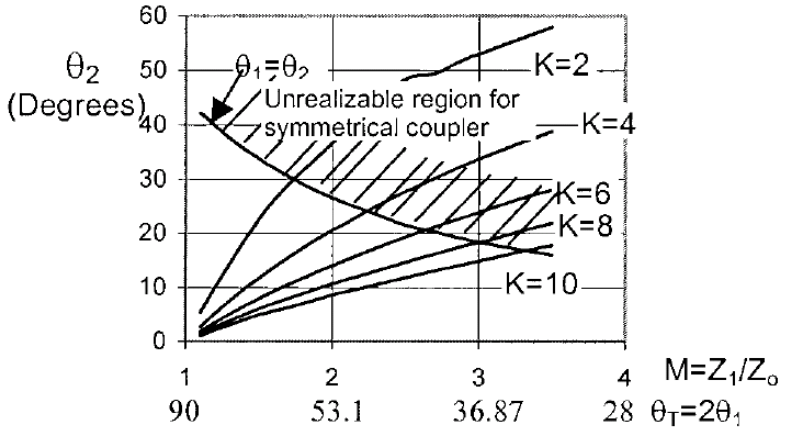

Figure C.2: Design curve for improved branchline using T-shaped transmission lines, [7]

Appendix D

Simulation Setups and Results

Some simulations and setups that are of less importance to the task, but still interesting for the reader are found in this appendix. These simulation result can be from for example intermediate stage simulations so that the reader can see results found on the way to the final stage.

D.1 Circuit 1 - Measurement and Simulation setup

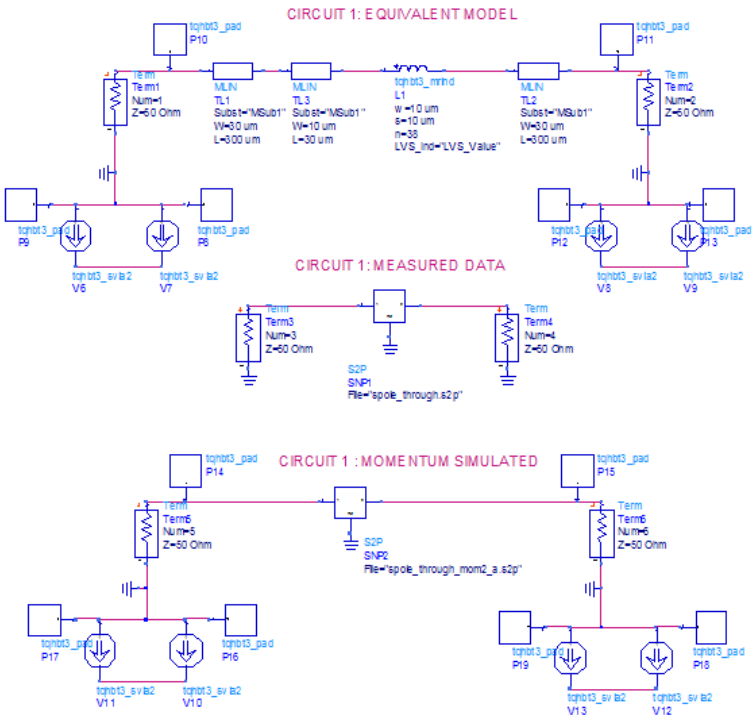

Figure D.1: Circuit 1: Simulation setup for comparison of equivalent model, Momentum simulated and Measured data

D.2 Improved Branch-Line Coupler - Simulations

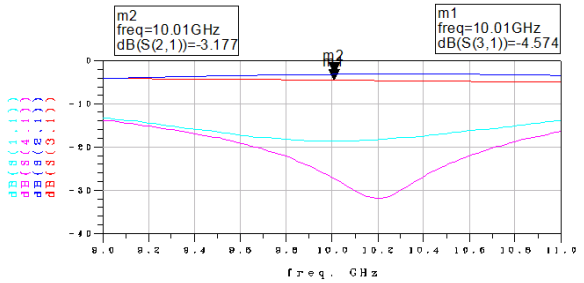

(a) S-parameter simulation

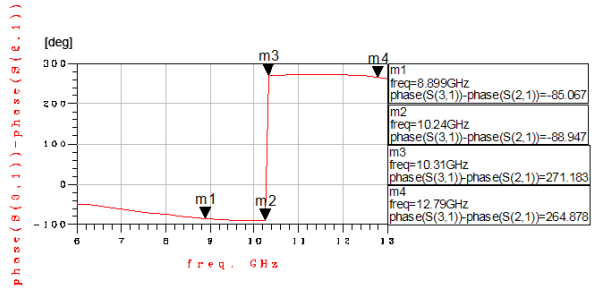

(b) Phase balance

Figure D.2: Schematic simulation results from Agilent ADS of the improved branch-line coupler

D.3 Topology 3 - Simulations

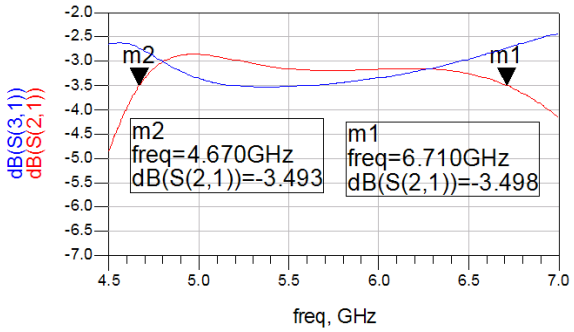

(a) Through(S_{21}) and coupled (S_{31}) results

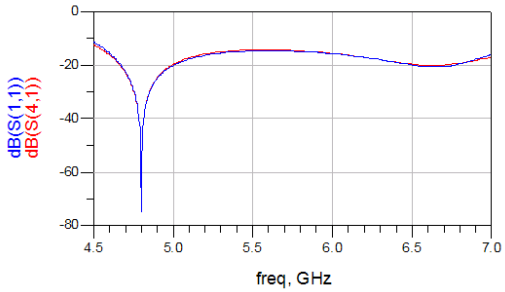

(b) Return loss(S_{11}) and isolation (S_{41}) results

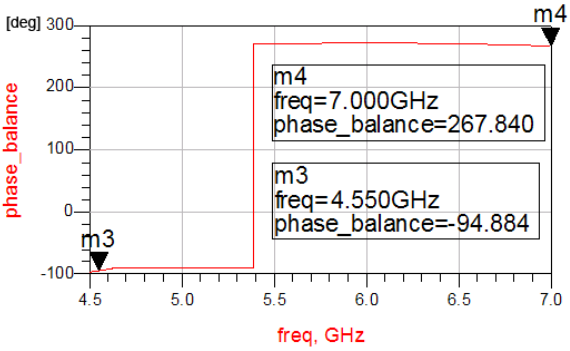

(c) Phase balance

Figure D.3: Simulation results using wide-band topology and eq. 5.18 with ideal components.